Am J Physiol Cell Physiol 308: C249–C263, 2015.
First published October 29, 2014; doi:10.1152/ajpcell.00265.2014.

Glucose and palmitate uncouple AMPK from autophagy in human aortic endothelial cells

Karen A. Weikel, José M. Cacicedo, Neil B. Ruderman, and Yasuo Ido

Department of Medicine, Boston University School of Medicine and Boston Medical Center, Boston, Massachusetts

Submitted 30 July 2014; accepted in final form 24 October 2014

Weikel KA, Cacicedo JM, Ruderman NB, Ido Y. Glucose and palmitate uncouple AMPK from autophagy in human aortic endothelial cells. *Am J Physiol Cell Physiol* 308: C249–C263, 2015. First published October 29, 2014; doi:10.1152/ajpcell.00265.2014.—Dysregulated autophagy and decreased AMP-activated protein kinase (AMPK) activity are each associated with atherogenesis. Atherogenesis is preceded by high circulating concentrations of glucose and fatty acids, yet the mechanism by which these nutrients regulate autophagy in human aortic endothelial cells (HAECs) is not known. Furthermore, whereas AMPK is recognized as an activator of autophagy in cells with few nutrients, its effects on autophagy in nutrient-rich HAECs has not been investigated. We maintained and passaged primary HAECs in media containing 25 mM glucose and incubated them subsequently with 0.4 mM palmitate. These conditions impaired basal autophagy and rendered HAECs more susceptible to apoptosis and adhesion of monocytes, outcomes attenuated by the autophagy activator rapamycin. Glucose and palmitate diminished AMPK activity and phosphorylation of the uncoordinated-51-like kinase 1 (ULK1) at Ser555, an autophagy-activating site targeted by AMPK. 5-Aminoimidazole-4-carboxamide-1-β-D-ribofuranoside (AICAR)-mediated activation of AMPK phosphorylated acetyl-CoA carboxylase, but treatment with AICAR or other AMPK activators (A769662, phenformin) did not restore ULK1 phosphorylation or autophagosome formation. To determine whether palmitate-induced ceramide accumulation contributed to this finding, we overexpressed a ceramide-metabolizing enzyme, acid ceramidase. The increase in acid ceramidase expression ameliorated the effects of excess nutrients on ULK1 phosphorylation, without altering the effects of the AMPK activators. Thus, unlike low nutrient conditions, AMPK becomes uncoupled from autophagy in HAECs in a nutrient-rich environment, such as that found in patients with increased cardiovascular risk. These findings suggest that combinations of AMPK-independent and AMPK-dependent therapies may be more effective alternatives than either therapy alone for treating nutrient-induced cellular dysfunction.

endothelium; autophagy; palmitate; glucose; AMPK

PATIENTS WITH THE METABOLIC SYNDROME or type 2 diabetes are more likely to develop cardiovascular complications such as atherosclerosis (26, 44, 54, 62, 77). Many cellular processes have been implicated in driving this pathology, but the predominant mechanisms remain unclear. Intriguing reports from humans and murine models of vascular disease indicate that dysregulation of macroautophagy, a pathway by which cellular components are recycled for energy utilization, may play a prominent role in this disease progression. Thus it has been shown that impairment of macroautophagy contributes to arterial aging (56), cardiomyocyte apoptosis (34), and aortic lesion formation (74).

Address for reprint requests and other correspondence: K. A. Weikel, Dept. of Medicine, Boston Univ. School of Medicine and Boston Medical Center,650 Albany St., Rm. 820, Boston, MA, 02118 (e-mail: karen.weikel@bmc.org).

Macroautophagy (hereinafter referred to as "autophagy") is a process by which cellular components are engulfed in a double-membraned vesicle, the autophagosome, and subsequently degraded by lysosomal proteases (17). Autophagy plays a key role in the cellular stress response, in which it can be induced by conditions such as starvation, inflammation, and oxidative stress (19, 51, 78). Regulation of starvation-induced autophagy is well-studied and involves complex signaling pathways that are modulated by the activities of several kinases including mammalian target of rapamycin complex 1 (mTORC1), uncoordinated-51-like kinase 1 (ULK1), and AMP-activated protein kinase (AMPK) (69, 89). Under low nutrient conditions, these kinases (among others) coordinate the formation of an autophagosome, to which autophagic substrates are recruited by adaptor proteins such as p62 (Fig. 1) (45). The autophagosome then fuses with a lysosome to create an autolysosome in which proteases, such as cathepsins, digest the target substrates along with their adaptor proteins (Fig. 1). Their breakdown products are then used to synthesize new proteins or fuel the cell (43).

A much less understood aspect of autophagy is regulation of its basal activity. Basal autophagy rids the cell of aged and damaged organelles when nutritional supply is not limited and is critical for cellular homeostasis in the vasculature as has been demonstrated by ApoE-null mice fed a Western diet (a model for atherosclerosis). Compared with wild-type mice, basal autophagy is impaired in the aorta of ApoE-null mice and its impairment in macrophages is associated with increased plaque development (74). These findings suggest that basal autophagy may be altered during atherosclerosis, but it remains to be determined how this type of autophagy is regulated and whether the same regulatory kinases and stimuli that modulate starvation-induced autophagy are involved. Importantly, it is not clear how hyperglycemia and dyslipidemia (specifically elevated free fatty acids), as observed in patients with type 2 diabetes and the metabolic syndrome, modulate basal autophagy in endothelial cells, the site of atherogenesis (3). Previous work in the pancreatic β-cell and macrophage has linked high concentrations of glucose and palmitate [a saturated fatty acid that has been associated with cellular toxicity (8, 9)] with autophagy inhibition (58, 88), but the ways in which these nutrients regulate basal autophagy in vascular tissues, such as human aortic endothelial cells (HAECs), have not been well characterized.

AMPK is a serine/threonine kinase that stimulates catabolic and inhibits anabolic processes to restore ATP levels when cellular energy is low (66). Activation of AMPK attenuates endothelial cell dysfunction (20) and aortic lesion formation (86) and also promotes starvation-induced autophagy through interactions with mTORC1 and/or ULK1 (Fig. 1) (21, 29, 42). It is not known, however, whether AMPK regulates basal

autophagy in the excess nutrient environment that predisposes endothelial cells to dysfunction and atherogenesis. Elucidation of this nutrient-AMPK-autophagy relationship in HAECs could be especially important since decreases in both AMPK activity and autophagy have been associated with an increased risk of atherosclerosis (20, 74, 86). An understanding of how hyperglycemia and dyslipidemia affect endothelial cell basal autophagy as well as the role of AMPK in this regulation could be critical for the development of pharmacological therapies that could target the endothelium to prevent atherogenesis. Thus, in the present study we first characterized autophagy in cultured primary HAECs incubated in high concentrations of glucose and palmitate, and then evaluated its regulation by AMPK.[1]

EXPERIMENTAL PROCEDURES

Materials. Human aortic endothelial cells (HAECs), human umbilical vein endothelial cells (HUVECs), and EGM-2 media (catalog no. cc-3162) were purchased from Lonza (Walkersville, MD). HEPES-buffered phenol red free media 199 (catalog no. M-2520, Sigma, St. Louis, MO), was supplemented with 5% FBS (catalog no. 26140-087, Life Technologies, Carlsbad, CA) and 50 μM carnitine (catalog no. C-0283, Sigma). Bafilomycin (catalog no. B1793), phenformin hydrochloride (catalog no. P7045), oleate (catalog no. O1008), and chloroform (catalog no. C7559) were also purchased from Sigma. Palmitate was purchased from Nu-Chek Prep (Elysian, MN). 5-Aminoimidazole-4-carboxamide-1-β-D-ribofuranoside (AICAR; catalog no. A611700) was purchased from Toronto Research Chemicals (North York, Ontario, Canada), and rapamycin (catalog no. R-5000) was purchased from LC Laboratories (Woburn, MA). A769662 (catalog no. 3336) was purchased from Tocris Biosciences (Minneapolis, MN). p62 antibody (catalog no. 610832) was purchased from BD Biosciences (San Jose, CA). Antibodies for LC3-II (catalog no. 3868S), phosphorylated (Thr172) AMPK(α1/α2) (catalog no. 2531S), phosphorylated (Ser79) acetyl-CoA carboxylase (ACC; catalog no. 3661S), ACC (catalog no. 4190S), phosphorylated (Thr 389) p70S6K (catalog no. 9205S), phosphorylated (Ser2448) mTOR (catalog no. 2971S), and phosphorylated (Ser555) ULK1 (catalog no. 5869S) were purchased from Cell Signaling Technology (Danvers, MA). Total AMPKα1 (catalog no. 3694-1) was purchased from Epitomics (Burlingame, CA). Total ULK1 (catalog no. sc-33182), mTOR (catalog no. 2972S), GAPDH (catalog no. sc-25778), and acid ceramidase (catalog no. sc-28486) antibodies were purchased from Santa Cruz Biotechnology (Dallas, TX). Actin antibody (catalog no. A4700) was purchased from Sigma (St. Louis, MO). Methanol (catalog no. A452-4) and acetic acid (catalog no. A38-212) were purchased from Fisher Scientific (Pittsburgh, PA). Secondary peroxidase-conjugated anti-mouse (catalog no. NXA931) and anti-rabbit (catalog no. NA934V) antibodies were purchased from GE Healthcare (Pittsburgh, PA). ^{32}P and [^{3}H]-L-serine were purchased from Perkin Elmer (Boston, MA).

Cell culture. HAECs were grown in EGM-2 media containing 2% FBS on Primaria culture dishes (reference no. 353803; BD Biosciences). For hyperglycemic conditions, cells were grown and passaged in EGM-2 media supplemented with D-glucose (catalog no. G-7021) (Sigma) to a final concentration of 25 mM. These cells were incubated in hyperglycemic media beginning in *passage 3* and when they reached 85% confluence were split in hyperglycemic media for *passage 4*. This protocol of maintaining and splitting the cells in hyperglycemic media was repeated for future passages. Because we are interested in modeling the long-term effects of hyperglycemia, rather than the transition to hyperglycemia, experiments using hyperglycemic cells began once they reached *passage 4*. At this stage, all of the cells were generated in a hyperglycemic environment and therefore exposed to it for their entire lifetime.

For both normoglycemic and hyperglycemic cells, experiments were performed when cells were 85–95% confluent. When applicable, HAECs were pretreated with the indicated concentrations of AICAR, A769662, phenformin, or rapamycin in EGM-2 for 30 min. Medium was then changed to DMEM (catalog no. 31600-034, Life Technologies) supplemented with 5% FBS containing either BSA, BSA-palmitate or BSA-oleate conjugates [3:1 free fatty acid (FFA):BSA ratio], as described previously (9). Briefly, BSA was used to both stabilize the insoluble fatty acids and transport them to the cell. Control-treated cells were exposed to media containing 0.5 mM BSA, while fatty acid-treated cells were exposed to media containing BSA conjugated to 0.4 mM palmitate or oleate at a 3:1 FFA:BSA molar ratio. Cells were exposed to BSA or BSA-fatty acid conjugates in DMEM for 6 h prior to harvesting for Western blotting, mRNA analysis, cathepsin L activity, and monocyte adhesion. For those experiments that included AICAR, A769662, phenformin, rapamycin, or bafilomycin, these compounds were also present in the DMEM for the 6 h incubation. Prior to TUNEL staining, cells were exposed to experimental conditions in DMEM for 16 h.

Western blotting. Cells were harvested and lysed in a Triton-based buffer containing 20 mM Tris pH 7.5, 150 mM NaCl, 1 mM EDTA, 1 mM EGTA, 0.1% SDS, 1% Triton X-100, 2.5 mM sodium pyrophosphate, 1 mM β-glycerophosphate, 1 mM sodium orthovanadate, and 1 μg/ml leupeptin. Proteins were separated using either 4–12% Bis-Tris gradient or 14% Tris-glycine gels (Life Technologies) and transferred to PVDF membranes. After blocking for at least 1 h at room temperature with nonfat milk, membranes were incubated in primary antibody overnight. Following washing in TBST, membranes were incubated in peroxidase-conjugated anti-mouse, anti-rabbit, or anti-goat antibodies and bands were visualized on film using Super-SignalWest Pico (catalog nos. 1856135 and 1856136) or Femto (catalog no. 34095) chemiluminescent substrate (Thermo Scientific, Rockford, IL). Densitometric analyses were carried out using Scion Image software and are presented after adjustment for expression of loading controls (actin or GAPDH).

Assessment of autophagosome formation. Cells were exposed to experimental conditions as described above for 6 h, in the presence or absence of 10 nM bafilomycin. Bafilomycin-induced LC3-II protein levels, or the ratio of LC3-II/LC3-I protein, as measured with Western blotting, were used as indicators of autophagosome abundance. To measure LC3-II protein accumulation by fluorescence microscopy, HAECs were infected with green fluorescent protein (GFP)-LC3-expressing lentivirus. Before comparing LC3-II puncta between treatments, we first set a threshold of "autophagy-induced LC3 accumulation," defined as the average pixel fluorescence in a single cell treated with rapamycin. Puncta fluorescence was visualized on a Nikon TE-200 Eclipse Inverted microscope (Melville, NY) and quantified with ImageJ (National Institutes of Health, Bethesda, MD). We then calculated the percentage of cells in each treatment group (control, control+bafilomycin, nutrient excess, nutrient excess+bafilomycin, nutrient excess+rapamycin, nutrient excess+rapamycin+bafilomycin, nutrient excess+AMPK activator, nutrient excess+AMPK activator+bafilomycin) that reached or surpassed this threshold. Bafilomycin-induced change in the percentage of cells above threshold was calculated for nutrient excess, nutrient excess+rapamycin and nutrient excess+AMPK activator conditions relative to control treatment.

Recombinant adenovirus and lentivirus. The adenovirus expressing a constitutively active mutant of AMPK ($\alpha 1_{312}T^{172}D$) was constructed from a truncated rat α_1-subunit with aspartate substituted for threonine 172, as described previously (41, 90). The adenovirus-expressing acid ceramidase was created as previously described (8). Lentivirus-expressing acid ceramidase (ASAH1, accession no. BC016481) was created by LR reaction of pENT221 (HsCD00039940, Harvard Plasmid) with a home-made lentivirus vector (containing a gateway cassette) to produce

[1] This article is the topic of an Editorial Focus by Wen-Xing Ding (19a).

a His-Flag tag at the COOH terminus of the protein. Infection of HAECs with adenovirus-expressing acid ceramidase had similar effects as infection with lentivirus-expressing acid ceramidase. The recombinant lentivirus plasmids expressing β-galactosidase and GFP-LC3 (Addgene no. 22418) were created in a home-made Gateway compatible lentivector after subcloning them into pENTR1A vector. All lentiviruses were produced as described previously (55).

Cathepsin L activity. Cathepsin L activity was measured using the Magic Red Cathepsin L Assay kit (catalog no. 941) purchased from Immunochemistry Technologies (Bloomington, MN) by following the manufacturer's instructions. Briefly, HAECs were treated with the indicated concentrations of glucose and palmitate along with a cresyl violet fluorophore that becomes fluorescent upon activation of cathepsin L. Cathepsin L activity was quantified on a Tecan microplate reader (San Jose, CA) and relative change in activity was calculated after adjusting for cell density and the number of acidic organelles.

AMPK activity assay. AMPK activity was measured as reported previously (30). In this assay, γ-^{32}P (catalog no. NEX011001MC, Perkin Elmer), ATP and *SAMS* peptide (HMRSAMSGLHLVKRR) were incubated with cell lysate. AMPK activity was assessed by measuring radioactive counts of ^{32}P following the reaction.

TUNEL staining. Cells were labeled using Roche's In Situ Cell Death Detection Kit, AP (catalog no. 11 684 809 910) (Indianapolis, IN) according to the manufacturer's instructions. TUNEL-positive staining was visualized using NBT-BCIP substrate (catalog no. 11 681 451 001) (Roche, Indianapolis, IN), and pictures were obtained on a Nikon TE-200 Eclipse Inverted microscope.

Real-time PCR. SYBR green Master Mix from Clontech (catalog no. RR420A; Mountain View, CA) was used to quantify real-time PCR product on Cepheid's Smart Cycler (Hamburg, PA). The following primers were used to detect mRNAs: β-actin: 5′-TTGTAACCA-ACTGGGACGATATGG-3′ (sense) and 5′-GATCTTGATCTTCAT-GGTGCTAGG-3′ (anti-sense); E-selectin: 5′-CTCTGACAGAAGA-AGCCAAG-3′ (sense), 5′-ACTTGAGTCCACTGAAGCCA-3′ (anti-sense). mRNA levels of E-selectin were quantified using the $2^{-\Delta\Delta}C_T$ method, relative to actin.

Monocyte adhesion. THP-1 monocytes (human cell line) were grown in RPMI-1640 media (catalog no. R-1383; Sigma) supplemented with D-glucose (13 mM final concentration) and 10% FBS. Monocytes were labeled with carboxyfluorescein succinimidyl ester (CFSE) dye (catalog no. C1157) (Life Technologies) and incubated with unsupplemented RPMI-1640 media for 30 min. Labeled monocytes were then incubated with HAECs for 1 h at 37°C. Unattached monocytes were washed off of HAECs with PBS, and the number of monocytes adherent to the HAECs were quantified using a microplate reader (Tecan).

Measurement of ceramide and sphingosine. HUVECs were incubated in M199 media containing either 5 or 30 mM glucose and either 0 or 0.3 mM palmitate (as indicated in Fig. 6*A*) as well as 2 mCi/ml [^{3}H]-L-serine for 16 h at 37°C. After measurement of specific activity in 100 ml of media, cells were washed three times with cold PBS. PBS (0.9 ml) containing 0.2% SDS was then added to each well, 100 μl of which was used to determine protein concentration. The remainder was transferred to fresh tubes, to which 3 ml CHCl3:MeOH (1:2, vol/vol) was added. One milliliter each of chloroform and water was then added and the sample was vortexed for 1 min. Samples were centrifuged for 5 min at 2,000 rpm to separate the phases, and the aqueous layer was aspirated while the organic phase was transferred to a new tube. Lipids were dried and resuspended in 50 μl CHCl3:MeOH (1:1). Ten micrograms of each standard were added to each tube and loaded onto a thin-layer chromatography plate and run in the solvent system [CHCl3:MeOH:3.5 N NH4OH (85:15:1)]. The bands were exposed to iodine and scraped into scintillation vials containing 1 ml MeOH:acetic acid (80:20). Samples were sonicated until bands dissolved. Four milliliters sonication fluid were added, and [^{3}H] was measured on a scintillation counter (3 min/vial).

Statistics. Data are presented as means ± SE. Unless stated otherwise, differences between treatment groups were analyzed using ANOVA, adjusting for multiple comparisons (GraphPad software, La Jolla, CA). $P < 0.05$ was considered significant.

RESULTS

In patients with poorly controlled type 2 diabetes, blood glucose levels are consistently elevated while fatty acid levels rise to peak concentrations during the 6–8 h of overnight fasting (27, 32, 68, 73, 75). Compared with control patients, free fatty acid levels in such patients with diabetes are 50% higher during overnight fast (68). Postprandial levels of palmitate (one of the predominant saturated fatty acids) in these patients have been reported to be nearly three times higher than healthy, nondiabetic subjects (68). To mimic this constant exposure of aortic endothelial cells to glucose interspersed with a subacute fatty acid (palmitate) exposure, we utilized a unique cell culture model to better understand the pathological effects of both of these nutrients on HAECs.

In our model, we sought to capture the long-term cellular effects of hyperglycemia, rather than the effects of a transition from normoglycemic (5 mM glucose) to hyperglycemic conditions (25 mM glucose). Therefore, HAECs destined for treatment with 25 mM glucose were switched from normoglycemic to hyperglycemic media beginning in *passage 3*. This medium was used for growth of these cells as well as their subsequent splitting into future generations. Experimental treatment and analysis of these cells began once the HAECs reached 95% confluence in *passage 4* (~10 days after beginning the use of the hyperglycemic media) and continued in future passages. Similar to the aortic endothelial cells of patients with poorly controlled type 2 diabetes, all of the cells beginning in the fourth passage of our model were generated in a hyperglycemic environment and therefore exposed to this stress for their entire lifetime ("chronic exposure").

To model the acute surges in palmitate experienced by patients with diabetes, we treated HAECs grown under hyperglycemic conditions with 0.4 mM palmitate [a physiologically relevant concentration that can be observed in diabetes patients during fasting or exercise (32, 75, 76)] for 6 h ("acute" exposure). Significant effects of palmitate were not observed with a shorter treatment (3 h), and longer incubations (24 and 48 h) did not augment the effects observed after 6 h.

Glucose with palmitate decreases autophagic flux in primary human aortic endothelial cells. Incubation of endothelial cells with high concentrations of glucose and fatty acids (including palmitate) has been shown to increase oxidative stress and inflammation (9, 41, 64), but their effects on autophagy in HAECs are not known. We began our investigation in HAECs by measuring protein levels of p62, a substrate adaptor protein that is degraded with its cargo by the autolysosome (Fig. 1). Thus, p62 protein accumulates when autophagy is impaired. Compared with HAECs incubated in control conditions (5 mM glucose, 0 mM palmitate), cells incubated in media with excess nutrients (chronic exposure to hyperglycemic media followed by a 6-h treatment with 0.4 mM palmitate) accumulated significantly more p62 protein (Fig. 2*A*). Preliminary data showed that either chronic exposure to glucose or acute exposure to palmitate also increased p62 protein levels, although not as robustly as when the nutrients were combined. Therefore, subsequent analyses of autophagy presented here were per-

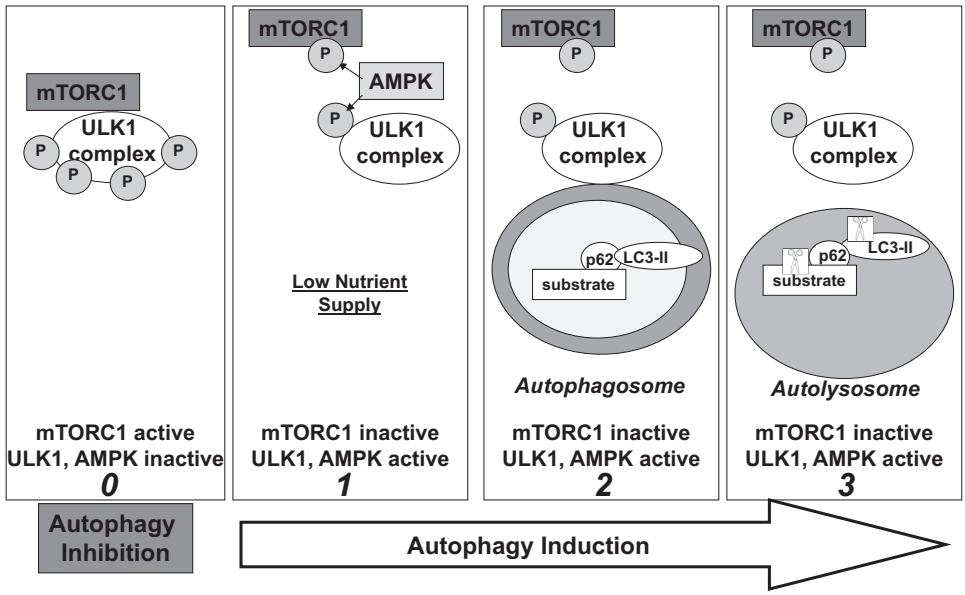

Fig. 1. Simplified model of starvation-induced autophagy. *Panel 0*: when mammalian target of rapamycin complex 1 (mTORC1) is active, it maintains uncoordinated-51-like kinase 1 (ULK1) in a hyperphosphorylated state that suppresses ULK1 activity and autophagy (89). *Panel 1*: activation of AMP-activated protein kinase (AMPK) under low nutrient conditions has been associated with phosphorylation of the raptor component of mTORC1, facilitating dissociation of mTORC1 from the ULK1 complex and activation of ULK1 (29, 42). AMPK can also activate ULK1 by phosphorylating Ser555 (21). *Panel 2*: ULK1 then translocates to the site of autophagosome membrane biogenesis. As the autophagosomal membrane elongates, microtubule-associated protein light chain 3 (LC3)-II binds to the inner membrane of the forming autophagosome and tethers p62 in complex with its substrate. *Panel 3*: once the autophagosome is formed, it fuses with the lysosome to create an autolysosome in which p62-substrate complexes and LC3-II are degraded by proteases (depicted as scissors in box) (89).

formed under the stress of both nutrients. Pretreatment with rapamycin, an inhibitor of mTORC1 (an enzyme that inhibits autophagy), ablated the nutrient-induced accumulation of p62, suggesting that under nutrient excess conditions, autophagy is impaired (Fig. 2*A*). Along with the saturated fatty acid palmitate, oleate, a monounsaturated fatty acid, is one of the most abundant fatty acids in circulation. We observed that HAECs exposed to elevated concentrations of glucose and oleate, instead of palmitate, did not accumulate p62, suggesting that all fatty acids do not impair autophagy (data not shown).

Glucose with palmitate impairs autophagosome formation and cathepsin L activity. Autophagosome formation, a fundamental step in autophagy (Fig. 1, *panels 1* and *2*), can be quantified indirectly by measuring the protein levels of microtubule-associated protein light chain 3 (LC3), a membrane-bound component of the autophagosomal membrane (Fig. 1) (89). LC3 is present in the cytosol as LC3-I (~16 kDa), but upon conjugation with phosphatidylethanolamine it is incorporated into the developing autophagosome membrane as LC3-II (Although the molecular weight of LC3-II exceeds that of LC3-I, LC3-II appears on SDS-PAGE at ~14 kDa due to its increased hydrophobicity.). Protein levels of LC3-II, or the LC3-II/LC3-I ratio (indicative of incorporation into the developing autophagosome) are surrogate indicators of autophagosome abundance and formation. Since LC3-II is continually turned over during autophagy, these measurements need to be performed in the presence of an autophagic inhibitor such as bafilomycin A1 (hereinafter referred to as simply bafilomycin) that prevents LC3-II degradation (50, 52). Thus, treatment with bafilomycin causes an accumulation of LC3-II protein. A decrease in bafilomycin-induced LC3-II protein accumulation would suggest that autophagosome formation is diminished.

We infected HAECs with lentivirus-expressing GFP-LC3 and measured LC3 puncta (indicative of autophagosomes) (50) in the presence of bafilomycin, using fluorescence microscopy. LC3 puncta were abundant in HAECs incubated in control conditions, but very few puncta accumulated in HAECs incubated in the presence of excess nutrients (Fig. 2*B*). Pretreatment of such HAECs with rapamycin restored LC3 puncta to levels observed in the control-treated cells (Fig. 2*B*). To confirm these findings, we used Western blotting to measure bafilomycin-induced LC3-II protein levels and the LC3-II/LC3-I ratio in HAECs incubated in control and nutrient excess conditions (Fig. 2*C*). Compared with control-treated cells, cells exposed to a nutrient excess showed decreased protein levels of both LC3-II and the LC3-II/LC3-I ratio (Fig. 2*C*, *lane 4* vs. *lane 2*). Similar to the data observed by microscopy, rapamycin treatment prevented nutrient-induced decreases in LC3 protein (Fig. 2*C*, *lane 6* vs. *lane 4*).

Following autophagosome formation, the autophagosome fuses with the lysosome to create an autolysosome that utilizes proteases such as cathepsins to degrade autophagic substrates (Fig. 1, *panel 3*). Palmitate has been shown to impair autophagy in pancreatic β-cells in part by inhibiting lysosomal protease activity (58). To determine whether HAECs are similarly affected, we measured the activity of cathepsin L, a lysosomal protease, in cells exposed to excesses of glucose and palmitate. As shown in Fig. 2*D*, chronic exposure of cells to high concentrations of these molecules decreased cathepsin L activity.

Glucose with palmitate increases apoptosis and inflammation in HAECs. When the autophagic pathway is blocked during the cellular stress response, cells may undergo apoptosis (6, 7). After observing that autophagy is impaired in HAECs treated with glucose and palmitate, we hypothesized that these cells also would be more susceptible to apoptosis. Relative to cells incubated in control conditions, those chronically exposed to high concentrations of glucose as well as a 16-h incubation with palmitate were more apoptotic, as indicated by increased TUNEL staining (Fig. 3*A*). Just as it restored autophagosome formation under nutrient excess conditions, rapamycin reduced this apoptotic response (Fig. 3*A*).

Apoptosis is the ultimate endothelial cell dysfunction and has been shown to predispose the vessel to the development of an atherosclerotic plaque (93). To better understand how nutrient-induced impairment of autophagy might contribute to apoptosis, we characterized an earlier indicator of endo-

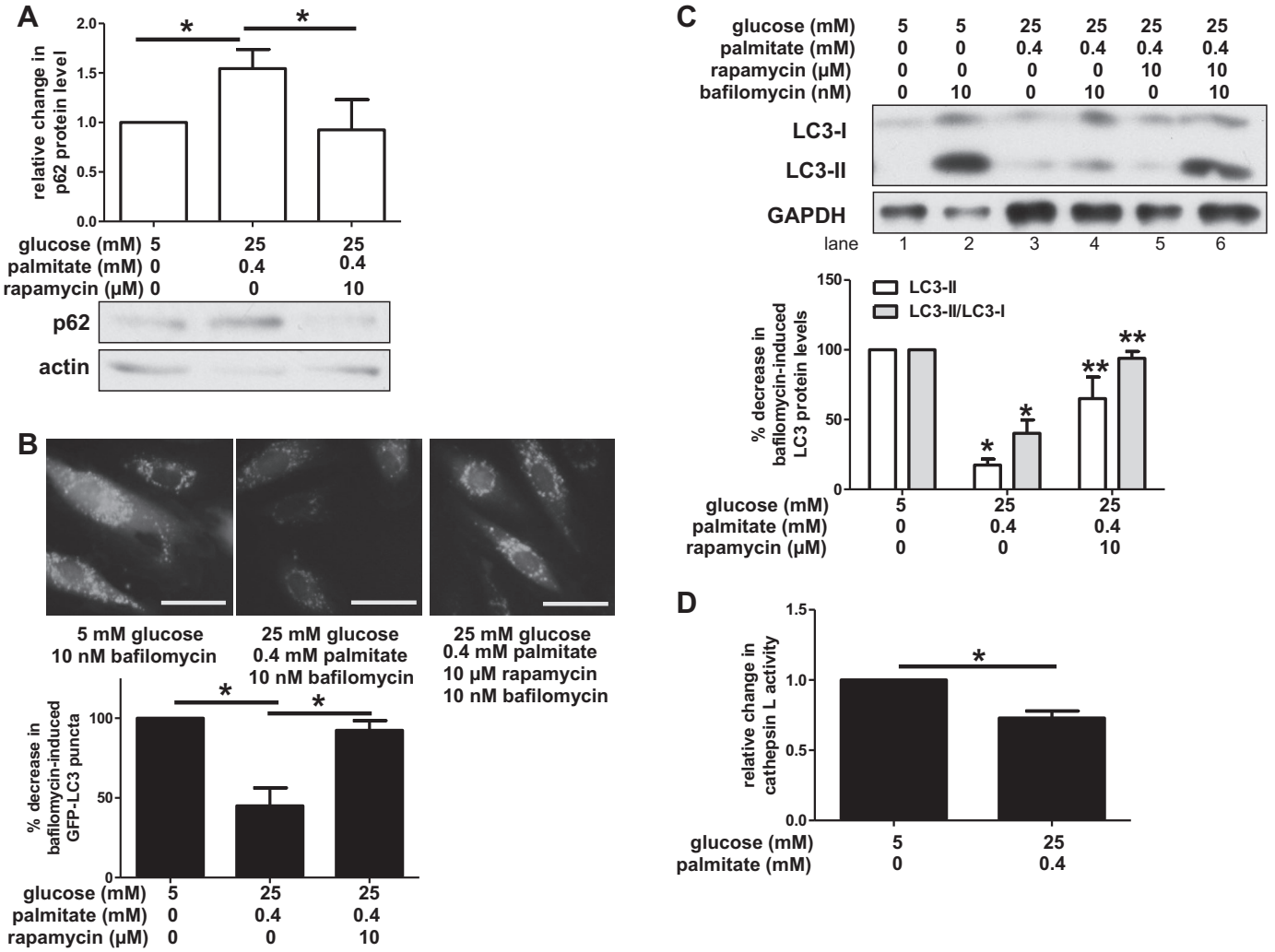

Fig. 2. Exposure to high concentrations of glucose and palmitate impairs autophagy. *A*: human aortic endothelial cells (HAECs) incubated in media containing high concentrations of glucose and palmitate increased levels of p62 protein, an autophagic substrate. Rapamycin, a chemical inducer of autophagy, attenuated p62 protein levels. A representative Western blot of lysates is shown for p62 and actin below a densitometric comparison of p62 protein levels (adjusted for loading control) ($n \geq 3$). *B*: green fluorescent protein (GFP)-LC3 puncta did not accumulate when HAECs were incubated in media containing high concentrations of glucose and palmitate, but treatment with rapamycin restored GFP-LC3 puncta. Bar, 50 μm. Bar graph below images shows quantification of changes in bafilomycin-induced GFP-LC3 puncta between treatment groups ($n = 3$). *C*: HAECs were incubated in media containing the indicated concentrations of glucose, palmitate, rapamycin, and bafilomycin. A representative Western blot is shown for LC3-I, LC3-II, and GAPDH. Quantification of changes in bafilomycin-induced LC3 protein levels between treatment groups is shown below as measured by LC3-II (relative to loading control) and the ratio of LC3-II/LC3-I ($n \geq 4$) *D*: HAECs were incubated in media containing the indicated concentrations of glucose and palmitate, along with a cresyl violet fluorophore that becomes fluorescent upon activation of cathepsin L. Cathepsin L activity was quantified on a microplate reader, and relative change in activity is shown after adjusting for cell density and the number of acidic organelles ($n = 4$). For *A*, *B*, and *D*, $^*P < 0.05$. For *C*, $^*P < 0.05$ compared with control conditions and $^{**}P < 0.05$ compared with nutrient excess conditions.

thelial dysfunction, inflammation, in HAECs exposed to excess nutrients. For this purpose, we measured the expression of E-selectin, a proinflammatory cytokine that facilitates the recruitment of mononuclear cells to the endothelium (23). Expression of E-selectin mRNA in cells incubated in a hyperglycemic media containing palmitate was slightly higher (albeit nonsignificantly, $P = 0.07$) than in control-treated cells, a response that was ablated by treatment with rapamycin (Fig. 3*B*). To determine whether these changes in E-selectin transcription might recruit more mononuclear cells to the endothelium, thus predisposing HAECs to inflammation and potential atherogenesis, we also assessed the adhesion of THP-1 monocytes to HAECs. As shown in Fig. 3*B*, incubation of HAECs in media containing excess glucose and palmitate increased the number of monocytes adherent to the HAECs, a clear indication that the endothelial cells became inflamed. Similar to its effects on E-selectin, rapamycin prevented this adhesion (Fig. 3*B*).

Glucose and palmitate decrease AMPK activity in HAECs. The data presented in Figs. 1–3 demonstrate that incubation of HAECs in high concentrations of palmitate and glucose decreases autophagy, increases inflammation, and predisposes the cells to apoptosis. Furthermore, both the inflammation and apoptosis were attenuated by rapamycin, an mTORC1 inhibitor that induces autophagy. This suggested that autophagy may be impaired in HAECs incubated in nutrient excess conditions because mTORC1 activity is increased. However, we did not

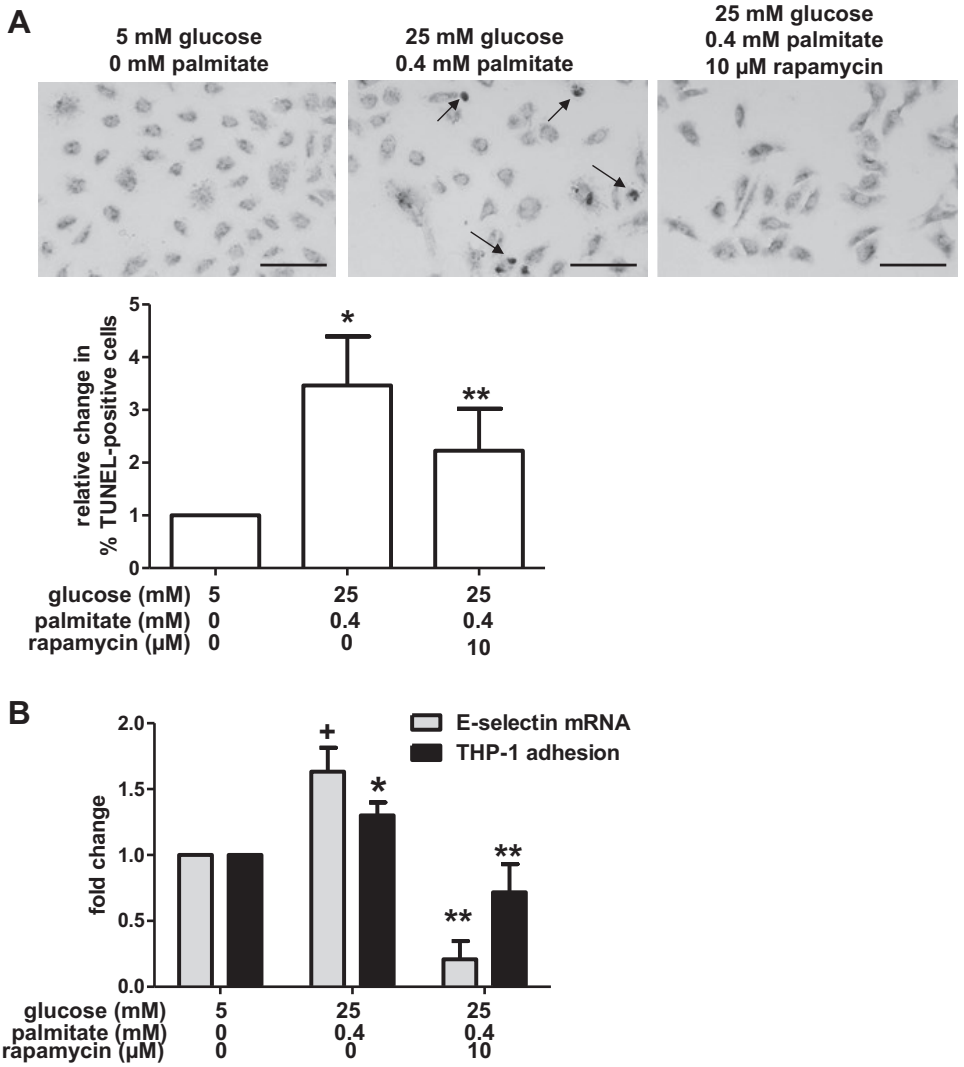

Fig. 3. Glucose and palmitate increase apoptosis and inflammation. *A*: HAECs were incubated in media containing the indicated concentrations of glucose, palmitate, and rapamycin. TUNEL staining was used to label DNA strand breaks, and they were visualized under brightfield microscopy. Punctate nuclear staining (arrows) indicates DNA strand breaks. Bar, 100 μm. The percentage of cells containing punctate nuclear staining ("TUNEL-positive") was calculated for each treatment group ($n = 5$ for control; $n = 5$ for excess nutrient; $n = 3$ for excess nutrient+ rapamycin). The graph indicates that excess nutrients increased the percentage of TUNEL-positive cells and that treatment with rapamycin attenuated these effects of glucose and palmitate on TUNEL staining. *B*: incubation of HAECs in media containing the indicated concentrations of glucose and palmitate also increased mRNA levels of the proinflammatory cytokine E-selectin ($n = 3$) and adhesion of THP-1 monocytes ($n = 9$) relative to control-treated cells. Treatment with rapamycin attenuated these changes. For *A* and *B*, $+P = 0.07$ and $*P \leq 0.05$ compared with control conditions; $**P < 0.05$ compared with excess nutrient conditions.

observe any increase in protein levels of phosphorylated (Thr 389) p70S6K nor the ratio of phosphorylated (Ser2448) mTOR/total mTOR protein (data not shown), two downstream targets of active mTORC1. Thus, we focused our attention on another kinase that has been reported to induce autophagy (at least under low nutrient conditions), AMPK. We hypothesized that autophagy impairment observed in the presence of high concentrations of glucose and palmitate could be due to decreased AMPK activity. We assessed AMPK activity in HAECs by measuring in vitro the phosphorylation of SAMS peptide (30) and in vivo the phosphorylation of AMPK on Thr172, a modification that is both required for AMPK activation and often used as a surrogate marker for its activity (12). Compared with control-treated cells, HAECs exposed to high concentrations of glucose and palmitate had reduced AMPK activity as demonstrated by both the SAMS peptide (Fig. 4*A*) and the Thr172 assays (Fig. 4*B*).

Activation of AMPK does not restore autophagy in a nutrient-laden environment. To address whether AMPK activity regulates nutrient-induced changes in autophagy in HAECs, we treated HAECs with AICAR, a chemical activator of AMPK, under control and excess nutrient conditions (81). We found that under both of these conditions, AICAR activated AMPK. AICAR increased protein levels of phosphorylated AMPK (Thr172) and also increased protein levels of phosphorylated acetyl-CoA carboxylase (ACC) at Ser79, a downstream target of AMPK (49) (Fig. 4, *C* and *D*). Since AICAR restored AMPK phosphorylation as well as that of its downstream target under nutrient excess conditions, we measured LC3 protein levels to determine whether autophagosome formation was also restored. Surprisingly, in the presence of high concentrations of glucose and palmitate, AICAR did not attenuate the loss of bafilomycin-induced LC3-II protein (Fig. 5, *A* and *B*, *lane 8* vs. *lane 6*). Similarly, it did not alleviate the effects of glucose and palmitate on the ratio of LC3-II/LC3-I or the appearance of GFP-LC3 puncta (data not shown). Unlike AICAR, which is metabolized to an AMP mimetic that activates AMPK, A769662 is an allosteric activator of AMPK (16). Treatment of HAECs with 10 μM A769662 increased phosphorylation of AMPK at Thr172 (data not shown), but like AICAR it did not restore LC3-II protein levels (Fig. 5, *A* and *C*, *lane 8* vs. *lane 6*), the ratio of LC3-II/LC3-I (data not shown), nor GFP-LC3 puncta (data not shown) in excess nutrient-exposed cells. Another chemical activator of AMPK, phenformin, is a biguanide and an analog of the diabetes drug metformin (33). As expected, treatment of HAECs with 1 mM

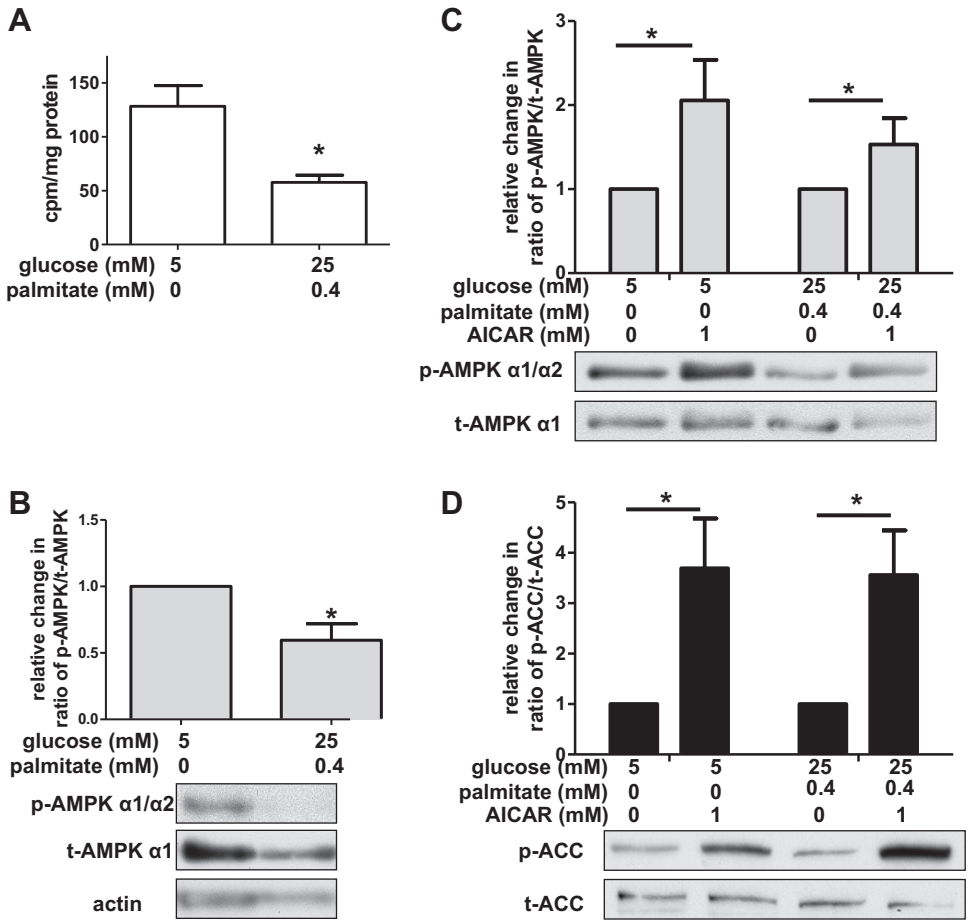

Fig. 4. Glucose and palmitate decrease AMPK activity in HAECs. *A*: AMPK activity was determined by SAMS peptide assay ($n = 8$), expressed in radiolabeled cpm/mg protein. *B*: relative change in the ratio of phosphorylated (Thr172) AMPK (p-AMPK α1/α2)/total AMPK (t-AMPK α1) protein is shown ($n = 6$) with a representative Western blot below the graph. *C*: densitometric analysis of the ratio of phosphorylated (Thr172) AMPK (p-AMPK α1/α2) to total AMPK (t-AMPK α1) protein indicates that aminoimidazole-4-carboxamide-1-β-4-ribofuranoside (AICAR) increases AMPK phosphorylation ($n \geq 5$). A representative Western blot is shown below the graph. *D*: densitometric analysis of the ratio of phosphorylated (Ser79) acetyl-CoA carboxylase (p-ACC)/total ACC (t-ACC) protein (a target of active AMPK) indicates activation of AMPK by AICAR ($n \geq 8$). A representative Western blot is shown below the graph. For *A* and *B*, $^*P < 0.05$ compared with control treatment, and for *C* and *D*, $^*P < 0.05$ for the effect of AICAR (two-way ANOVA).

phenformin increased phosphorylation of AMPK at Thr172 (data not shown). Similar to the effects observed with AICAR and A769662, phenformin treatment did not significantly attenuate nutrient-induced changes in LC3 protein levels (Fig. 5, *A* and *D*, *lane 8* vs. *lane 6* and data not shown). Nutrient-induced changes in LC3 protein levels were also not affected by infection of HAECs with an adenovirus-expressing ($\alpha 1_{312}T^{172}D$) AMPK, a mutant form of AMPK that is constitutively active (data not shown) (41, 90). Compared with activation of AMPK by chemical activators, AMPK activation with this mutant was minimal.

mTORC1, AMPK, and ULK1 interact in a complex, dynamic relationship to modulate starvation-induced autophagy (1). ULK1 can be inactivated via mTORC1-dependent phosphorylation (Fig. 1, *panel 0*). When mTORC1 activity declines, it dissociates from ULK1, perhaps enabling autophagy-inducing kinases such as AMPK to activate ULK1 (Fig. 1, *panel 1*). A number of studies have shown that Ser555 on ULK1 is a target of AMPK and that its phosphorylation is required for starvation-induced autophagy (21, 29, 48, 60, 88). To address the dissociation between AMPK activation and autophagosome formation in HAECs exposed to nutrient excess conditions, we measured the effect of these nutrients on phosphorylation of Ser555 on ULK1. We found that, compared with control-treated cells, HAECs exposed to nutrient excess conditions had lower protein levels of phosphorylated ULK1 (Ser555) (Fig. 5*E*). This suggests that in HAECs, phosphorylation of ULK1 at Ser555 is an important feature of basal autophagy induction. In addition to Ser555, we found that incubation of cells with glucose and palmitate also decreased ULK1 phosphorylation at Ser317, another target of AMPK (data not shown) (48). Treatment of nutrient-laden HAECs with AICAR, A769662, or phenformin to activate AMPK did not restore ULK1 phosphorylation at Ser555 (Fig. 5*E*) nor did expression of a constitutively active AMPK (data not shown). AICAR also did not restore ULK1 phosphorylation at Ser317 (data not shown). These data suggest that a combined treatment of glucose with palmitate affects the AMPK-ULK1 and AMPK-ACC signaling pathways differently.

Overexpression of acid ceramidase restores nutrient-induced losses in ULK1 phosphorylation at Ser555. To address the question of why AMPK is uncoupled from autophagy signaling in the presence of excess glucose and palmitate, we drew on our observation that palmitate, but not oleate, exposure was associated with impaired autophagy (as indicated by an accumulation of p62 protein) (Fig. 2*A* and data not shown). One of the differences between these two fatty acids is that only palmitate contributes to the cellular synthesis of ceramide, a lipid species that has been shown to decrease AMPK activity and contribute to vascular dysfunction (91, 94). Ceramide and its metabolite, sphingosine-1-phosphate, have been suggested to have opposing roles in autophagy regulation, but whether ceramide accumulation induces or impairs basal autophagy in HAECs remains unclear (70, 84). Since ceramide may potentially regulate both AMPK and autophagy, we hypothesized that, in the presence of palmitate, ceramides may prevent

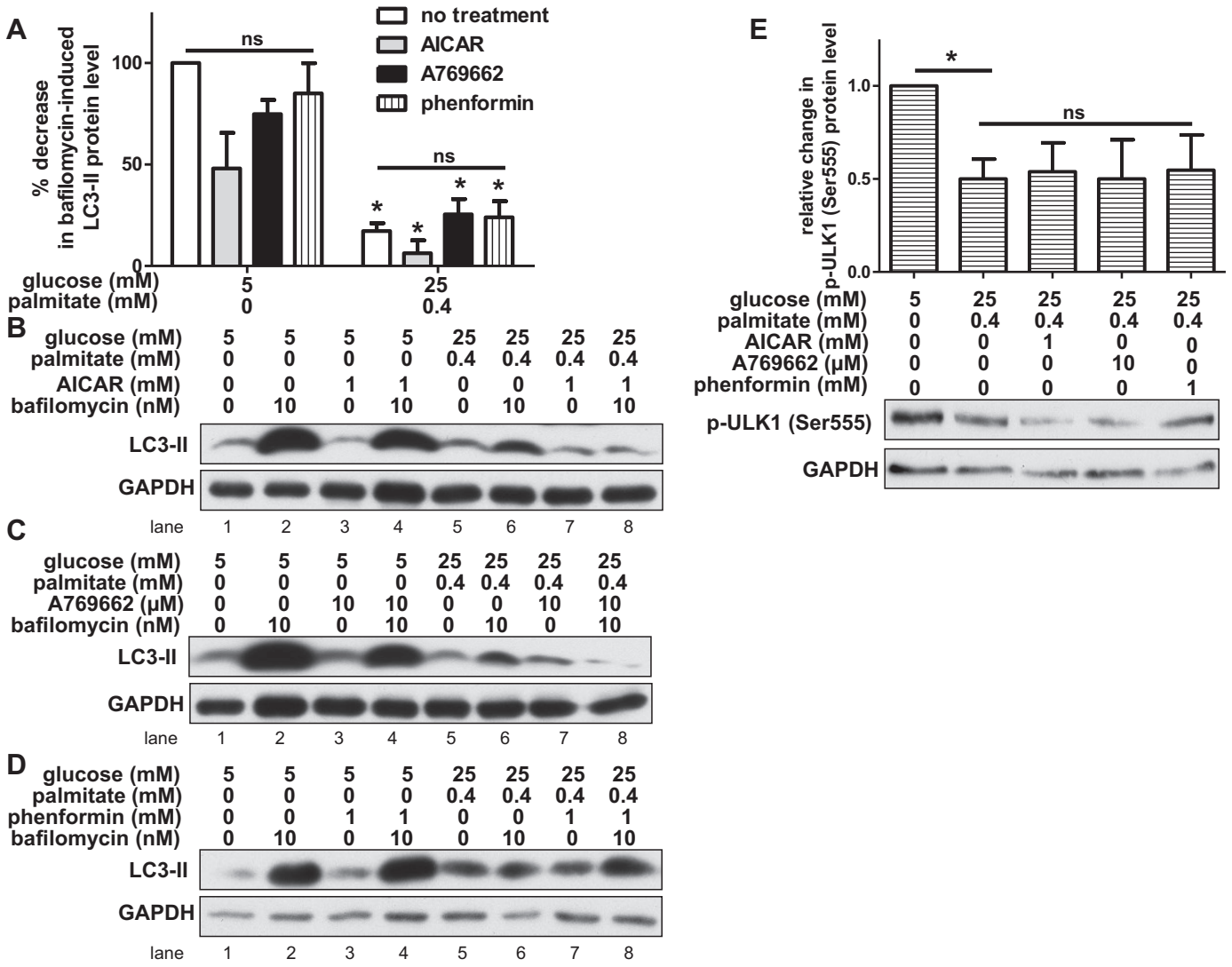

Fig. 5. Chemical activation of AMPK does not restore autophagy in HAECs exposed to glucose and palmitate. *A*: bafilomycin-induced LC3-II protein levels (relative to loading control) were measured by Western blot in HAECs incubated with 1 mM AICAR, 10 μM A769662, 1 mM phenformin, or no activator. Relative to cells incubated in control conditions, the percent decrease in LC3-II protein level is shown for cells incubated in nutrient excess conditions ($n \geq 3$). *$P < 0.05$ relative to control conditions; ns, no significant effect of AMPK activators within each treatment condition. *B–D*: LC3-II and GAPDH protein bands are shown on representative Western blots for AICAR (*B*), A769662 (*C*), and phenformin (*D*) treatments. *E*: the relative change (after adjusting for loading control) in protein level of phosphorylated ULK1 (p-ULK1 Ser555), an autophagy-activating site targeted by AMPK, is shown ($n \geq 4$). A representative Western blot is shown for p-ULK1 (Ser555) and GAPDH below. *$P < 0.05$; ns, no significant effect of AMPK activators in the excess nutrient condition.

activated AMPK from phosphorylating ULK1 and inducing autophagy.

Previous work from our laboratory indicated that palmitate treatment increased ceramides in retinal pericytes (8). As an extension of this finding, we sought to determine whether macrovascular endothelial cells had a similar response. To perform the radioactive tracer experiments and thin-layer chromatography required to resolve ceramides and their related lipid intermediates, a very large number of cells was required per sample. This posed a challenge since HAECs are notoriously poor growers. Thus, we used HUVECs, which can be readily expanded to large quantities. We found that incubation of HUVECs in 0.3 mM palmitate increased ceramide generation (Fig. 6*A*). Furthermore, ceramide generation also increased in HUVECs incubated in 30 mM glucose or a combination of glucose with palmitate (Fig. 6*A*). Ceramides are utilized by many cells for the synthesis of a number of different structural and signaling lipid species including sphingosine (the precursor to sphingosine-1-phosphate), glucosylceramides, and sphingomyelin (57). We also found this to be the case in HUVECs, as high concentrations of glucose and palmitate increased intracellular generation of sphingosine (Fig. 6*A*).

Conversion of ceramide to sphingosine is catalyzed by a lysosomal enzyme, acid ceramidase (57). Overexpression of acid ceramidase prevents palmitate-induced accumulation of ceramides (14), while its impairment results in ceramide accumulation (38). To assess the potential role of nutrient-induced ceramides in modulation of the phosphorylation of ULK1, we ectopically expressed acid ceramidase in HAECs (Fig. 6*B*).

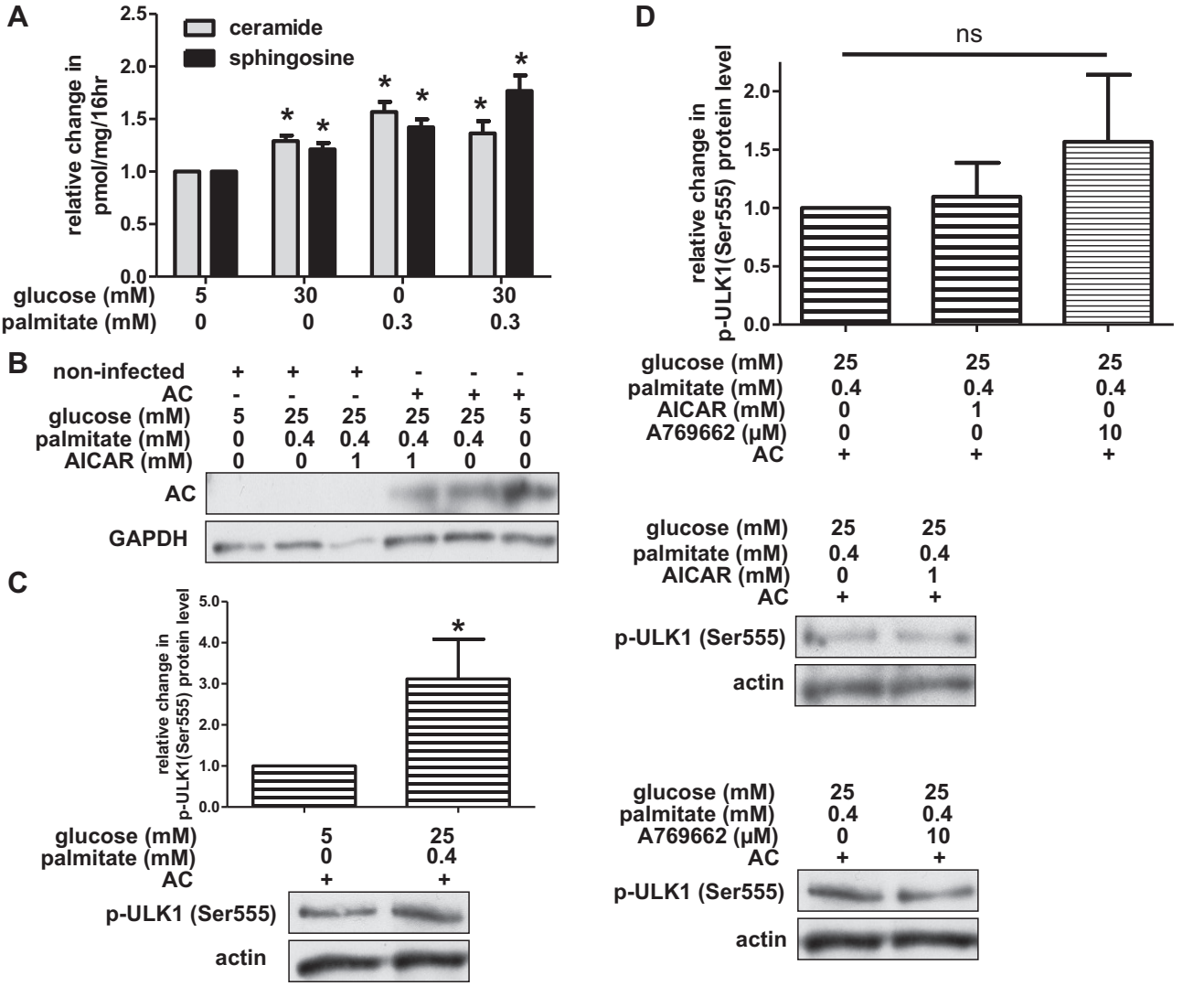

Fig. 6. Overexpression of acid ceramidase (AC) restores ULK1 phosphorylation. *A*: human umbilical vein endothelial cells (HUVECs) were incubated in media containing glucose and/or palmitate for 16 h, and ceramide and sphingosine levels were measured using [^{3}H]-L-serine (adjusted for protein content). Data are expressed as change in ceramide or sphingosine levels for each treatment group relative to control-treated cells ($n \geq 3$). *B*: noninfected HAECs and HAECs infected with acid ceramidase lentivirus were incubated in media containing glucose, palmitate, and AICAR. Acid ceramidase expression was evaluated by Western blotting. *C*: HAECs ectopically expressing acid ceramidase were incubated in control or nutrient excess conditions. Densitometric analysis of p-ULK1 (Ser555) protein level (relative to loading control) is shown ($n = 6$) with representative Western blot below. *D*: HAECs ectopically expressing acid ceramidase were incubated in media containing high concentrations of glucose and palmitate as well as AICAR or A769662. Densitometric analysis of p-ULK1 (Ser555) protein level (relative to loading control) is shown ($n = 3$) with representative Western blots below. For *A*, *C*, and *D*, $^*P < 0.05$ compared with control conditions; ns, no significant difference.

Unlike noninfected (and β-galactosidase-infected) HAECs in which glucose and palmitate treatment decreased phosphorylation of ULK1 at Ser555 (Fig. 5*E* and data not shown), HAECs overexpressing acid ceramidase had higher levels of phosphorylated ULK1 when incubated with excess glucose and palmitate (Fig. 6*C* and data not shown). In this nutrient-laden context, treatment of these cells with AICAR or A769662 did not further increase expression of phosphorylated ULK1 (Fig. 6*D*). These data suggest that, in the presence of glucose and palmitate, accumulation of ceramides (which would be diminished by acid ceramidase overexpression) may inhibit ULK1 phosphorylation but may not contribute to uncoupling between AMPK and ULK1.

Interestingly, ectopic expression of acid ceramidase restored ULK1 phosphorylation in a nutrient-laden environment, but it did not restore LC3 protein levels (data not shown), alter the effects of AMPK activators on LC3 (data not shown), nor reduce accumulation of p62 protein in nutrient-laden HAECs (data not shown). This indicates that while ceramides may be important regulators of ULK1, the latter is not the only contributor to autophagy regulation under these conditions.

DISCUSSION

Regulation of AMPK plays a key role in events associated with type 2 diabetes and the metabolic syndrome, as well as their associated cardiovascular complications (24, 87). For example, two of the most widely prescribed drugs for diabetes and cardiovascular disease, metformin and statins, are both

AMPK activators (82, 95). While these treatments significantly help control diabetes and reduce cardiovascular risk across the population, they are not effective in all patients (10, 37, 79). This suggests that there may be certain pathological conditions in which AMPK becomes uncoupled from its expected cellular actions. Under these conditions (such as the model described here), there may be a need for additional therapeutic targets independent of AMPK.

In this study, we treated primary HAECs with a combination of high glucose and palmitate to model the pathological stress of poorly controlled type 2 diabetes. In this context, we analyzed the role of AMPK in regulation of autophagy, a pathological process implicated in atherogenesis. Consistent with the role of these nutrients in endothelial dysfunction (22, 47) as well as previous studies in HUVECs (8, 9, 41), we found that the combination of glucose and palmitate both predisposed HAECs to apoptosis and increased their inflammatory profile. The subsequent novel findings from our work were as follows: *1*) Incubation of HAECs with the same high concentrations of glucose and palmitate that increased apoptosis and inflammation also impaired autophagy. *2*) Exposure of HAECs to excess nutrients decreased the activity of AMPK. *3*) Unlike low nutrient conditions, chemical activation of AMPK did not restore autophagy in this nutrient-laden environment. *4*) Ectopic expression of acid ceramidase prevented nutrient-induced decreases in ULK1 phosphorylation at Ser555, an AMPK-targeted site. Surprisingly, increased expression of acid ceramidase did not alter the effects of AICAR, A769662, or phenformin on ULK1 phosphorylation. This suggests that accumulation of ceramides may directly regulate ULK1, but perhaps not through interfering with the actions of AMPK. Collectively, these data indicate that, in HAECs, high concentrations of glucose and palmitate exert a metabolic stress (perhaps similar to those of patients who do not respond to AMPK activators) under which AMPK activation does not induce autophagy. Intriguingly, restoration of ULK1 phosphorylation by acid ceramidase expression suggests that targeting ceramide or its metabolites may be a potential alternative target to allay nutrient-induced stress in the endothelium.

The complex interactions between ULK1, AMPK, and mTORC1 that regulate starvation-induced autophagy are incompletely understood, but even less is known about their relationships when there is an excess of nutrients (13, 63). The inability to restore autophagic flux in HAECs by chemically activating AMPK contrasts with previous observations in rodent myocardial cells (34) and macrophages (88). He and colleagues (34) observed that hyperglycemia, induced by streptozotocin or incubating myoblasts in a high-glucose media (30 mM for 48 h), suppressed autophagy; likewise Wen and colleagues found that 24 h of exposure to 0.5 mM palmitate, following stimulation with lipopolysaccharide, suppressed autophagy in rodent macrophages (88). In each of these contexts, autophagy impairment induced by a single nutrient was overcome by AMPK activation. AMPK activation in our human endothelial cell model may have been insufficient to rescue nutrient-induced loss of autophagy due to the presence of a double nutrient (glucose with palmitate), rather than a single nutrient (glucose or palmitate)-induced inhibition of flux. The increased severity of a double nutrient—compared with a single nutrient—stress is supported by data from the β-cell, in which a combined exposure to glucose and palmitate produced a more severe inhibition of autophagic flux than exposure to palmitate alone (58). In addition to the presence of a double nutrient stress, our model differs from the above mentioned studies in its use of a chronic glucose treatment. Exposure of HAECs to high concentrations of glucose during cell division and throughout the lifetime of the newly generated cells may alter their epigenetic profile, as shown in other types of cells (67), thus altering their responses to chemical activators such as AICAR.

Given that acid ceramidase expression did not facilitate additional ULK1 phosphorylation or autophagosome formation with AICAR or A769662, the mechanism by which glucose and palmitate alter the interaction between AMPK and autophagy remains an open area of investigation. There may be separate pools of AMPK in which signaling to its respective targets (ACC or ULK1) is differentially regulated. This could be a result of glucose- and palmitate-induced posttranslational modifications on AMPK and/or ULK1 that prevent interactions between these two molecules. Interestingly, in the presence of excess nutrients, acid ceramidase expression restored phosphorylation of ULK1 (Fig. 6*C* and data not shown) and ACC, but not AMPK (data not shown), suggesting that acid ceramidase may be involved in both of these signaling pathways, perhaps independent of AMPK. There are several potential mechanisms by which ceramides or other sphingolipid metabolites may be impairing autophagy, including activation of protein phosphatases (65, 85) and increased levels of endoplasmic reticulum stress (5, 28, 61). Further study is needed to focus on the contribution of these lipids, as well as other processes such as the inhibition of Sirtuin-1 (SIRT1) (31, 53, 59, 83) or generation of oxidative stress (78) to nutrient-induced autophagy impairment.

In addition to modulating the initiation stages of autophagy through ULK1, excess nutrients may also affect initiation and autophagosomal membrane elongation through inhibition of SIRT1, an NAD^+-dependent histone deacetylase. We and others have shown that high concentrations of glucose or palmitate impair AMPK activity (35, 36, 91) as well as SIRT1 activity (2, 18, 71, 80). AMPK and SIRT1 have also been shown to regulate one another (11, 39, 55). In the nucleus, SIRT1 may activate autophagy by deacetylating several members of the forkhead family of transcription factors, FOXO1 and FOXO3 (31, 53). In the cytosol, *in vitro* studies indicate that Atg5, Atg7, and Atg8, autophagy proteins required for the formation and elongation of the autophagosomal membrane (46), are also targets of SIRT1 (59). In mouse embryonic fibroblasts, overexpression of wild-type SIRT1, but not deacetylase-deficient SIRT1, increased basal autophagy (59). Consistent with this autophagy-activating characteristic of SIRT1, inhibition of SIRT1 in human THP-1 cells impaired autophagy (83).

Perhaps related to SIRT1 inhibition, excess concentrations of glucose and palmitate may also impair autophagy through the generation of oxidative stress (4, 8, 15, 40, 72). Reactive oxygen species inhibit the activity of Atg4 (78), an enzyme required both for the maturation of LC3 prior to its incorporation into the forming autophagosomal membrane and for LC3 cleavage from the outside of the autolysosome to be recycled for future use (46). Thus, inhibition of Atg4 via

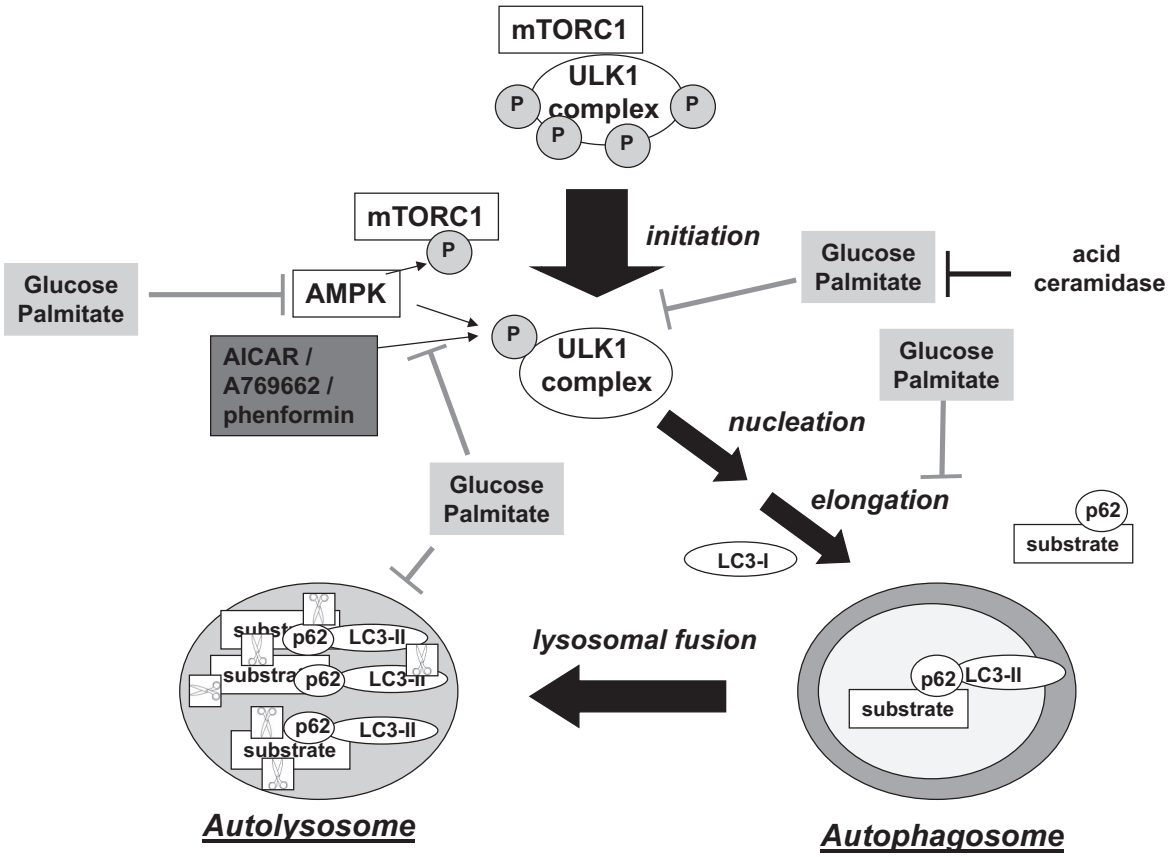

Fig. 7. Excess nutrients impair autophagic flux and uncouple AMPK from autophagy. Established regulators of starvation-induced autophagy are depicted in white boxes whereas effects of excess nutrients are shown in light gray. High concentrations of glucose and palmitate decrease phosphorylation of ULK1 at Ser555, impair autophagosome formation, and decrease lysosomal protease activity, resulting in an overall decrease in autophagic flux. Glucose and palmitate also reduce AMPK activity, but chemical activation of AMPK does not restore ULK1 phosphorylation or autophagosome formation in the presence of these nutrients. Overexpression of acid ceramidase restores ULK1 phosphorylation, suggesting that ceramides are involved in nutrient-induced regulation of ULK1.

reactive oxygen species may impair the incorporation of both newly synthesized and recycled LC3 into autophagosomes. LC3 is critical for the elongation of the autophagosomal membrane and depletion of LC3 has been associated with smaller autophagosomes (92), which would consequently degrade fewer substrates.

In addition to decreasing autophagosome size, glucose and palmitate may also impair substrate degradation in the autolysosome by interfering with lysosomal proteases, such as cathepsin L (Fig. 2*D*). Evidence from pancreatic β-cells and hepatocytes suggests that nutrient-induced loss of degradative capacity may be due to inhibition of lysosomal acidification (58) or increased lysosomal permeabilization (25).

In summary, we have identified autophagic dysregulation as a new mechanism linking glucose and palmitate exposure with inflammation and apoptosis in HAECs. Our HAEC model of poorly controlled type 2 diabetes, which utilizes chronic exposure to glucose in combination with acute palmitate treatment, revealed that these nutrients impair ULK1 phosphorylation, autophagosome formation, and cathepsin L activity (Fig. 7). Similar to the effects of glucose and palmitate on AMPK activity in rat adipocytes (35), cardiomyocytes (36), and bovine aortic endothelial cells (91), we found that these nutrients decreased AMPK activity in HAECs. However, activation of AMPK was not sufficient to restore autophagy in this nutrient-rich environment. Thus, unlike the role ascribed to AMPK in starvation-induced autophagy, AMPK is uncoupled from autophagy under nutrient excess conditions. Rather than exclusively targeting AMPK, ceramide or its metabolites may be additional targets for therapies aimed at preventing autophagic dysregulation in excess nutrient conditions. Moreover, an improved understanding of the particular types and magnitudes of stress under which AMPK activation can restore cellular homeostasis and those in which it cannot, may lay the foundation for improved treatments for a variety of metabolic pathologies in which AMPK plays a critical role.

GRANTS

Research support was provided by National Heart, Lung, and Blood Institute Grant PO1 HL-068758 and National Institute of Diabetes and Digestive and Kidney Diseases Grant T32 DK-007201 from National Institutes of Health (to N. B. Ruderman).

DISCLOSURES

No conflicts of interest, financial or otherwise, are declared by the author(s).

AUTHOR CONTRIBUTIONS

K.A.W. and Y.I. conception and design of research; K.A.W. and Y.I. performed experiments; K.A.W. and Y.I. analyzed data; K.A.W. and Y.I. interpreted results of experiments; K.A.W. prepared figures; K.A.W. drafted

manuscript; K.A.W., J.M.C., N.B.R., and Y.I. edited and revised manuscript; K.A.W., J.M.C., N.B.R., and Y.I. approved final version of manuscript.

REFERENCES

1. **Alers S, Loffler AS, Wesselborg S, Stork B.** Role of AMPK-mTOR-Ulk1/2 in the regulation of autophagy: cross talk, shortcuts, and feedbacks. *Mol Cell Biol* 32: 2–11, 2012.
2. **Arunachalam G, Samuel SM, Marei I, Ding H, Triggle CR.** Metformin modulates hyperglycaemia-induced endothelial senescence and apoptosis through SIRT1. *Br J Pharmacol* 171: 523–535, 2014.
3. **Bornfeldt KE, Tabas I.** Insulin resistance, hyperglycemia, and atherosclerosis. *Cell Metab* 14: 575–585, 2011.
4. **Borradaile NM, Pickering JG.** Nicotinamide phosphoribosyltransferase imparts human endothelial cells with extended replicative lifespan and enhanced angiogenic capacity in a high glucose environment. *Aging Cell* 8: 100–112, 2009.
5. **Boslem E, MacIntosh G, Preston AM, Bartley C, Busch AK, Fuller M, Laybutt DR, Meikle PJ, Biden TJ.** A lipidomic screen of palmitate-treated MIN6 beta-cells links sphingolipid metabolites with endoplasmic reticulum (ER) stress and impaired protein trafficking. *Biochem J* 435: 267–276, 2011.
6. **Boya P, Gonzalez-Polo RA, Casares N, Perfettini JL, Dessen P, Larochette N, Metivier D, Meley D, Souquere S, Yoshimori T, Pierron G, Codogno P, Kroemer G.** Inhibition of macroautophagy triggers apoptosis. *Mol Cell Biol* 25: 1025–1040, 2005.
7. **Bursch W.** The autophagosomal-lysosomal compartment in programmed cell death. *Cell Death Differ* 8: 569–581, 2001.
8. **Cacicedo JM, Benjachareowong S, Chou E, Ruderman NB, Ido Y.** Palmitate-induced apoptosis in cultured bovine retinal pericytes: roles of NAD(P)H oxidase, oxidant stress, and ceramide. *Diabetes* 54: 1838–1845, 2005.
9. **Cacicedo JM, Yagihashi N, Keaney JF Jr, Ruderman NB, Ido Y.** AMPK inhibits fatty acid-induced increases in NF-kappaB transactivation in cultured human umbilical vein endothelial cells. *Biochem Biophys Res Commun* 324: 1204–1209, 2004.
10. **Cairns SA, Shalet S, Marshall AJ, Hartog M.** A comparison of phenformin and metformin in the treatment of maturity onset diabetes. *Diabete Metab* 3: 183–188, 1977.
11. **Canto C, Gerhart-Hines Z, Feige JN, Lagouge M, Noriega L, Milne JC, Elliott PJ, Puigserver P, Auwerx J.** AMPK regulates energy expenditure by modulating NAD+ metabolism and SIRT1 activity. *Nature* 458: 1056–1060, 2009.
12. **Cardaci S, Filomeni G, Ciriolo MR.** Redox implications of AMPK-mediated signal transduction beyond energetic clues. *J Cell Sci* 125: 2115–2125, 2012.
13. **Chan EY.** Regulation and function of uncoordinated-51 like kinase proteins. *Antioxid Redox Signal* 17: 775–785, 2012.
14. **Chavez JA, Holland WL, Bar J, Sandhoff K, Summers SA.** Acid ceramidase overexpression prevents the inhibitory effects of saturated fatty acids on insulin signaling. *J Biol Chem* 280: 20148–20153, 2005.
15. **Chinen I, Shimabukuro M, Yamakawa K, Higa N, Matsuzaki T, Noguchi K, Ueda S, Sakanashi M, Takasu N.** Vascular lipotoxicity: endothelial dysfunction via fatty-acid-induced reactive oxygen species overproduction in obese Zucker diabetic fatty rats. *Endocrinology* 148: 160–165, 2007.
16. **Cool B, Zinker B, Chiou W, Kifle L, Cao N, Perham M, Dickinson R, Adler A, Gagne G, Iyengar R, Zhao G, Marsh K, Kym P, Jung P, Camp HS, Frevert E.** Identification and characterization of a small molecule AMPK activator that treats key components of type 2 diabetes and the metabolic syndrome. *Cell Metab* 3: 403–416, 2006.
17. **De Duve C, Wattiaux R.** Functions of lysosomes. *Annu Rev Physiol* 28: 435–492, 1966.
18. **de Kreutzenberg SV, Ceolotto G, Papparella I, Bortoluzzi A, Semplicini A, Dalla Man C, Cobelli C, Fadini GP, Avogaro A.** Downregulation of the longevity-associated protein sirtuin 1 in insulin resistance and metabolic syndrome: potential biochemical mechanisms. *Diabetes* 59: 1006–1015, 2010.
19. **Deretic V.** Autophagy: an emerging immunological paradigm. *J Immunol* 189: 15–20, 2012.

19a. **Ding WX.** *Uncoupling AMPK from autophagy: a foe that hinders the beneficial effects of metformin treatment on metabolic syndrome-associated atherosclerosis?* Focus on "Glucose and palmitate uncouple AMPK from autophagy in human aortic endothelial cells." *Am J Physiol Cell Physiol* (December 10, 2014). doi:10.1152/ajpcell.00375.2014.

20. **Dong Y, Zhang M, Wang S, Liang B, Zhao Z, Liu C, Wu M, Choi HC, Lyons TJ, Zou MH.** Activation of AMP-activated protein kinase inhibits oxidized LDL-triggered endoplasmic reticulum stress in vivo. *Diabetes* 59: 1386–1396, 2010.
21. **Egan DF, Shackelford DB, Mihaylova MM, Gelino S, Kohnz RA, Mair W, Vasquez DS, Joshi A, Gwinn DM, Taylor R, Asara JM, Fitzpatrick J, Dillin A, Viollet B, Kundu M, Hansen M, Shaw RJ.** Phosphorylation of ULK1 (hATG1) by AMP-activated protein kinase connects energy sensing to mitophagy. *Science* 331: 456–461, 2011.
22. **El-Awady MS, El-Agamy DS, Suddek GM, Nader MA.** Propolis protects against high glucose-induced vascular endothelial dysfunction in isolated rat aorta. *J Physiol Biochem* 70: 247–254, 2014.
23. **Eringa EC, Serne EH, Meijer RI, Schalkwijk CG, Houben AJ, Stehouwer CD, Smulders YM, van Hinsbergh VW.** Endothelial dysfunction in (pre)diabetes: characteristics, causative mechanisms and pathogenic role in type 2 diabetes. *Rev Endocr Metab Disord* 14: 39–48, 2013.
24. **Eurich DT, McAlister FA, Blackburn DF, Majumdar SR, Tsuyuki RT, Varney J, Johnson JA.** Benefits and harms of antidiabetic agents in patients with diabetes and heart failure: systematic review. *BMJ* 335: 497, 2007.
25. **Feldstein AE, Werneburg NW, Li Z, Bronk SF, Gores GJ.** Bax inhibition protects against free fatty acid-induced lysosomal permeabilization. *Am J Physiol Gastrointest Liver Physiol* 290: G1339–G1346, 2006.
26. **Feskens EJ, Kromhout D.** Glucose tolerance and the risk of cardiovascular disease: the Zutphen Study. *J Clin Epidemiol* 45: 1327–1334, 1992.
27. **Fredrickson DS, Gordon RS, Ono K, Cherkes A.** The metabolism of albumin-bound C14-labeled unesterified fatty acids in normal human subjects. *J Clin Invest* 37: 1504, 1958.
28. **Gonzalez-Rodriguez A, Mayoral R, Agra N, Valdecantos MP, Pardo V, Miquilena-Colina ME, Vargas-Castrillon J, Lo Iacono O, Corazzari M, Fimia GM, Piacentini M, Muntane J, Bosca L, Garcia-Monzon C, Martin-Sanz P, Valverde AM.** Impaired autophagic flux is associated with increased endoplasmic reticulum stress during the development of NAFLD. *Cell Death Dis* 5: e1179, 2014.
29. **Gwinn DM, Shackelford DB, Egan DF, Mihaylova MM, Mery A, Vasquez DS, Turk BE, Shaw RJ.** AMPK phosphorylation of raptor mediates a metabolic checkpoint. *Mol Cell* 30: 214–226, 2008.
30. **Hardie DG, Salt IP, Davies SP.** Analysis of the role of the AMP-activated protein kinase in the response to cellular stress. *Methods Mol Biol* 99: 63–74, 2000.
31. **Hariharan N, Maejima Y, Nakae J, Paik J, Depinho RA, Sadoshima J.** Deacetylation of FoxO by Sirt1 plays an essential role in mediating starvation-induced autophagy in cardiac myocytes. *Circ Res* 107: 1470–1482, 2010.
32. **Havel RJ, Naimark A, Borchgrevink CF.** Turnover rate and oxidation of free fatty acids of blood plasma in man during exercise: studies during continuous infusion of palmitate-1–C14. *J Clin Invest* 42: 1054–1063, 1963.
33. **Hawley SA, Boudeau J, Reid JL, Mustard KJ, Udd L, Makela TP, Alessi DR, Hardie DG.** Complexes between the LKB1 tumor suppressor, STRAD alpha/beta and MO25 alpha/beta are upstream kinases in the AMP-activated protein kinase cascade. *J Biol* 2: 28, 2003.
34. **He C, Zhu H, Li H, Zou MH, Xie Z.** Dissociation of Bcl-2-Beclin1 complex by activated AMPK enhances cardiac autophagy and protects against cardiomyocyte apoptosis in diabetes. *Diabetes* 62: 1270–1281, 2013.
35. **Hebbachi A, Saggerson D.** Acute regulation of 5′-AMP-activated protein kinase by long-chain fatty acid, glucose and insulin in rat primary adipocytes. *Biosci Rep* 33: 71–82, 2012.
36. **Hickson-Bick DL, Buja LM, McMillin JB.** Palmitate-mediated alterations in the fatty acid metabolism of rat neonatal cardiac myocytes. *J Mol Cell Cardiol* 32: 511–519, 2000.
37. **Hoeg JM, Brewer HB Jr.** 3-Hydroxy-3-methylglutaryl–coenzyme A reductase inhibitors in the treatment of hypercholesterolemia. *JAMA* 258: 3532–3536, 1987.
38. **Holland WL, Miller RA, Wang ZV, Sun K, Barth BM, Bui HH, Davis KE, Bikman BT, Halberg N, Rutkowski JM, Wade MR, Tenorio VM, Kuo MS, Brozinick JT, Zhang BB, Birnbaum MJ, Summers SA, Scherer PE.** Receptor-mediated activation of ceramidase activity initiates the pleiotropic actions of adiponectin. *Nat Med* 17: 55–63, 2011.
39. **Hou X, Xu S, Maitland-Toolan KA, Sato K, Jiang B, Ido Y, Lan F, Walsh K, Wierzbicki M, Verbeuren TJ, Cohen RA, Zang M.** SIRT1

regulates hepatocyte lipid metabolism through activating AMP-activated protein kinase. *J Biol Chem* 283: 20015–20026, 2008.

40. **Huang C, Lin MZ, Cheng D, Braet F, Pollock CA, Chen XM.** Thioredoxin-interacting protein mediates dysfunction of tubular autophagy in diabetic kidneys through inhibiting autophagic flux. *Lab Invest* 94: 309–320, 2014.
41. **Ido Y, Carling D, Ruderman N.** Hyperglycemia-induced apoptosis in human umbilical vein endothelial cells: inhibition by the AMP-activated protein kinase activation. *Diabetes* 51: 159–167, 2002.
42. **Inoki K, Zhu T, Guan KL.** TSC2 mediates cellular energy response to control cell growth and survival. *Cell* 115: 577–590, 2003.
43. **Itakura E, Kishi-Itakura C, Mizushima N.** The hairpin-type tail-anchored SNARE syntaxin 17 targets to autophagosomes for fusion with endosomes/lysosomes. *Cell* 151: 1256–1269, 2012.
44. **Jax TW.** Metabolic memory: a vascular perspective. *Cardiovasc Diabetol* 9: 51, 2010.
45. **Johansen T, Lamark T.** Selective autophagy mediated by autophagic adapter proteins. *Autophagy* 7: 279–296, 2011.
46. **Kaufmann A, Beier V, Franquelim HG, Wollert T.** Molecular mechanism of autophagic membrane-scaffold assembly and disassembly. *Cell* 156: 469–481, 2014.
47. **Kim F, Tysseling KA, Rice J, Pham M, Haji L, Gallis BM, Baas AS, Paramsothy P, Giachelli CM, Corson MA, Raines EW.** Free fatty acid impairment of nitric oxide production in endothelial cells is mediated by IKKbeta. *Arterioscler Thromb Vasc Biol* 25: 989–994, 2005.
48. **Kim J, Kundu M, Viollet B, Guan KL.** AMPK and mTOR regulate autophagy through direct phosphorylation of Ulk1. *Nat Cell Biol* 13: 132–141, 2011.
49. **Kim KH, Lopez-Casillas F, Bai DH, Luo X, Pape ME.** Role of reversible phosphorylation of acetyl-CoA carboxylase in long-chain fatty acid synthesis. *FASEB J* 3: 2250–2256, 1989.
50. **Klionsky DJ, Abdalla FC, Abeliovich H, Abraham RT, Acevedo-Arozena A, Adeli K, Agholme L, Agnello M, Agostinis P, Aguirre-Ghiso JA, Ahn HJ, Ait-Mohamed O, Ait-Si-Ali S, Akematsu T, Akira S, Al-Younes HM, Al-Zeer MA, Albert ML, Albin RL, Alegre-Abarrategui J, Aleo MF, Alirezaei M, Almasan A, Almonte-Becerril M, Amano A, Amaravadi R, Amarnath S, Amer AO, Andrieu-Abadie N, Anantharam V, Ann DK, Anoopkumar-Dukie S, Aoki H, Apostolova N, Arancia G, Aris JP, Asanuma K, Asare NY, Ashida H, Askanas V, Askew DS, Auberger P, Baba M, Backues SK, Baehrecke EH, Bahr BA, Bai XY, Bailly Y, Baiocchi R, Baldini G, Balduini W, Ballabio A, Bamber BA, Bampton ET, Banhegyi G, Bartholomew CR, Bassham DC, Bast RC, Jr, Batoko H, Bay BH, Beau I, Bechet DM, Begley TJ, Behl C, Behrends C, Bekri S, Bellaire B, Bendall LJ, Benetti L, Berliocchi L, Bernardi H, Bernassola F, Besteiro S, Bhatia-Kissova I, Bi X, Biard-Piechaczyk M, Blum JS, Boise LH, Bonaldo P, Boone DL, Bornhauser BC, Bortoluci KR, Bossis I, Bost F, Bourquin JP, Boya P, Boyer-Guittaut M, Bozhkov PV, Brady NR, Brancolini C, Brech A, Brenman JE, Brennand A, Bresnick EH, Brest P, Bridges D, Bristol ML, Brookes PS, Brown EJ, Brumell JH, Brunetti-Pierri N, Brunk UT, Bulman DE, Bultman SJ, Bultynck G, Burbulla LF, Bursch W, Butchar JP, Buzgariu W, Bydlowski SP, Cadwell K, Cahova M, Cai D, Cai J, Cai Q, Calabretta B, Calvo-Garrido J, Camougrand N, Campanella M, Campos-Salinas J, Candi E, Cao L, Caplan AB, Carding SR, Cardoso SM, Carew JS, Carlin CR, Carmignac V, Carneiro LA, Carra S, Caruso RA, Casari G, Casas C, Castino R, Cebollero E, Cecconi F, Celli J, Chaachouay H, Chae HJ, Chai CY, Chan DC, Chan EY, Chang RC, Che CM, Chen CC, Chen GC, Chen GQ, Chen M, Chen Q, Chen SS, Chen W, Chen X, Chen YG, Chen Y, Chen YJ, Chen Z, Cheng A, Cheng CH, Cheng Y, Cheong H, Cheong JH, Cherry S, Chess-Williams R, Cheung ZH, Chevet E, Chiang HL, Chiarelli R, Chiba T, Chin LS, Chiou SH, Chisari FV, Cho CH, Cho DH, Choi AM, Choi D, Choi KS, Choi ME, Chouaib S, Choubey D, Choubey V, Chu CT, Chuang TH, Chueh SH, Chun T, Chwae YJ, Chye ML, Ciarcia R, Ciriolo MR, Clague MJ, Clark RS, Clarke PG, Clarke R, Codogno P, Coller HA, Colombo MI, Comincini S, Condello M, Condorelli F, Cookson MR, Coombs GH, Coppens I, Corbalan R, Cossart P, Costelli P, Costes S, Coto-Montes A, Couve E, Coxon FP, Cregg JM, Crespo JL, Cronje MJ, Cuervo AM, Cullen JJ, Czaja MJ, D'Amelio M, Darfeuille-Michaud A, Davids LM, Davies FE, De Felici M, de Groot JF, de Haan CA, De Martino L, De Milito A, De Tata V, Debnath J, Degterev A, Dehay B, Delbridge LM, Demarchi F, Deng YZ, Dengjel J, Dent P, Denton D, Deretic V, Desai SD, Devenish RJ, Di Gioacchino M, Di Paolo G, Di Pietro C, Diaz-Araya G, Diaz-Laviada I, Diaz-Meco MT, Diaz-Nido J, Dikic I, Dinesh-Kumar SP, Ding WX, Distelhorst CW, Diwan A, Djavaheri-Mergny M, Dokudovskaya S, Dong Z, Dorsey FC, Dosenko V, Dowling JJ, Doxsey S, Dreux M, Drew ME, Duan Q, Duchosal MA, Duff K, Dugail I, Durbeej M, Duszenko M, Edelstein CL, Edinger AL, Egea G, Eichinger L, Eissa NT, Ekmekcioglu S, El-Deiry WS, Elazar Z, Elgendy M, Ellerby LM, Eng KE, Engelbrecht AM, Engelender S, Erenpreisa J, Escalante R, Esclatine A, Eskelinen EL, Espert L, Espina V, Fan H, Fan J, Fan QW, Fan Z, Fang S, Fang Y, Fanto M, Fanzani A, Farkas T, Farre JC, Faure M, Fechheimer M, Feng CG, Feng J, Feng Q, Feng Y, Fesus L, Feuer R, Figueiredo-Pereira ME, Fimia GM, Fingar DC, Finkbeiner S, Finkel T, Finley KD, Fiorito F, Fisher EA, Fisher PB, Flajolet M, Florez-McClure ML, Florio S, Fon EA, Fornai F, Fortunato F, Fotedar R, Fowler DH, Fox HS, Franco R, Frankel LB, Fransen M, Fuentes JM, Fueyo J, Fujii J, Fujisaki K, Fujita E, Fukuda M, Furukawa RH, Gaestel M, Gailly P, Gajewska M, Galliot B, Galy V, Ganesh S, Ganetzky B, Ganley IG, Gao FB, Gao GF, Gao J, Garcia L, Garcia-Manero G, Garcia-Marcos M, Garmyn M, Gartel AL, Gatti E, Gautel M, Gawriluk TR, Gegg ME, Geng J, Germain M, Gestwicki JE, Gewirtz DA, Ghavami S, Ghosh P, Giammarioli AM, Giatromanolaki AN, Gibson SB, Gilkerson RW, Ginger ML, Ginsberg HN, Golab J, Goligorsky MS, Golstein P, Gomez-Manzano C, Goncu E, Gongora C, Gonzalez CD, Gonzalez R, Gonzalez-Estevez C, Gonzalez-Polo RA, Gonzalez-Rey E, Gorbunov NV, Gorski S, Goruppi S, Gottlieb RA, Gozuacik D, Granato GE, Grant GD, Green KN, Gregorc A, Gros F, Grose C, Grunt TW, Gual P, Guan JL, Guan KL, Guichard SM, Gukovskaya AS, Gukovsky I, Gunst J, Gustafsson AB, Halayko AJ, Hale AN, Halonen SK, Hamasaki M, Han F, Han T, Hancock MK, Hansen M, Harada H, Harada M, Hardt SE, Harper JW, Harris AL, Harris J, Harris SD, Hashimoto M, Haspel JA, Hayashi S, Hazelhurst LA, He C, He YW, Hebert MJ, Heidenreich KA, Helfrich MH, Helgason GV, Henske EP, Herman B, Herman PK, Hetz C, Hilfiker S, Hill JA, Hocking LJ, Hofman P, Hofmann TG, Hohfeld J, Holyoake TL, Hong MH, Hood DA, Hotamisligil GS, Houwerzijl EJ, Hoyer-Hansen M, Hu B, Hu CA, Hu HM, Hua Y, Huang C, Huang J, Huang S, Huang WP, Huber TB, Huh WK, Hung TH, Hupp TR, Hur GM, Hurley JB, Hussain SN, Hussey PJ, Hwang JJ, Hwang S, Ichihara A, Ilkhanizadeh S, Inoki K, Into T, Iovane V, Iovanna JL, Ip NY, Isaka Y, Ishida H, Isidoro C, Isobe K, Iwasaki A, Izquierdo M, Izumi Y, Jaakkola PM, Jaattela M, Jackson GR, Jackson WT, Janji B, Jendrach M, Jeon JH, Jeung EB, Jiang H, Jiang JX, Jiang M, Jiang Q, Jiang X, Jimenez A, Jin M, Jin S, Joe CO, Johansen T, Johnson DE, Johnson GV, Jones NL, Joseph B, Joseph SK, Joubert AM, Juhasz G, Juillerat-Jeanneret L, Jung CH, Jung YK, Kaarniranta K, Kaasik A, Kabuta T, Kadowaki M, Kagedal K, Kamada Y, Kaminskyy VO, Kampinga HH, Kanamori H, Kang C, Kang KB, Kang KI, Kang R, Kang YA, Kanki T, Kanneganti TD, Kanno H, Kanthasamy AG, Kanthasamy A, Karantza V, Kaushal GP, Kaushik S, Kawazoe Y, Ke PY, Kehrl JH, Kelekar A, Kerkhoff C, Kessel DH, Khalil H, Kiel JA, Kiger AA, Kihara A, Kim DR, Kim DH, Kim EK, Kim HR, Kim JS, Kim JH, Kim JC, Kim JK, Kim PK, Kim SW, Kim YS, Kim Y, Kimchi A, Kimmelman AC, King JS, Kinsella TJ, Kirkin V, Kirshenbaum LA, Kitamoto K, Kitazato K, Klein L, Klimecki WT, Klucken J, Knecht E, Ko BC, Koch JC, Koga H, Koh JY, Koh YH, Koike M, Komatsu M, Kominami E, Kong HJ, Kong WJ, Korolchuk VI, Kotake Y, Koukourakis MI, Kouri Flores JB, Kovacs AL, Kraft C, Krainc D, Kramer H, Kretz-Remy C, Krichevsky AM, Kroemer G, Kruger R, Krut O, Ktistakis NT, Kuan CY, Kucharczyk R, Kumar A, Kumar R, Kumar S, Kundu M, Kung HJ, Kurz T, Kwon HJ, La Spada AR, Lafont F, Lamark T, Landry J, Lane JD, Lapaquette P, Laporte JF, Laszlo L, Lavandero S, Lavoie JN, Layfield R, Lazo PA, Le W, Le Cam L, Ledbetter DJ, Lee AJ, Lee BW, Lee GM, Lee J, Lee JH, Lee M, Lee MS, Lee SH, Leeuwenburgh C, Legembre P, Legouis R, Lehmann M, Lei HY, Lei QY, Leib DA, Leiro J, Lemasters JJ, Lemoine A, Lesniak MS, Lev D, Levenson VV, Levine B, Levy E, Li F, Li JL, Li L, Li S, Li W, Li XJ, Li YB, Li YP, Liang C, Liang Q, Liao YF, Liberski PP, Lieberman A, Lim HJ, Lim KL, Lim K, Lin CF, Lin FC, Lin J, Lin JD, Lin K, Lin WW, Lin WC, Lin YL, Linden R, Lingor P, Lippincott-Schwartz J, Lisanti MP, Liton PB, Liu B, Liu CF, Liu K, Liu L, Liu QA, Liu W, Liu YC, Liu Y, Lockshin RA, Lok CN, Lonial S, Loos B, Lopez-Berestein G, Lopez-Otin C, Lossi L, Lotze MT, Low P, Lu B, Lu Z, Luciano F, Lukacs NW, Lund AH, Lynch-Day MA, Ma Y, Macian F, MacKeigan JP, Macleod KF, Madeo F, Maiuri L, Maiuri MC, Malagoli D,**

Malicdan MC, Malorni W, Man N, Mandelkow EM, Manon S, Manov I, Mao K, Mao X, Mao Z, Marambaud P, Marazziti D, Marcel YL, Marchbank K, Marchetti P, Marciniak SJ, Marcondes M, Mardi M, Marfe G, Marino G, Markaki M, Marten MR, Martin SJ, Martinand-Mari C, Martinet W, Martinez-Vicente M, Masini M, Matarrese P, Matsuo S, Matteoni R, Mayer A, Mazure NM, McConkey DJ, McConnell MJ, McDermott C, McDonald C, McInerney GM, McKenna SL, McLaughlin B, McLean PJ, McMaster CR, McQuibban GA, Meijer AJ, Meisler MH, Melendez A, Melia TJ, Melino G, Mena MA, Menendez JA, Menna-Barreto RF, Menon MB, Menzies FM, Mercer CA, Merighi A, Merry DE, Meschini S, Meyer CG, Meyer TF, Miao CY, Miao JY, Michels PA, Michiels C, Mijaljica D, Milojkovic A, Minucci S, Miracco C, Miranti CK, Mitroulis I, Miyazawa K, Mizushima N, Mograbi B, Mohseni S, Molero X, Mollereau B, Mollinedo F, Momoi T, Monastyrska I, Monick MM, Monteiro MJ, Moore MN, Mora R, Moreau K, Moreira PI, Moriyasu Y, Moscat J, Mostowy S, Mottram JC, Motyl T, Moussa CE, Muller S, Munger K, Munz C, Murphy LO, Murphy ME, Musaro A, Mysorekar I, Nagata E, Nagata K, Nahimana A, Nair U, Nakagawa T, Nakahira K, Nakano H, Nakatogawa H, Nanjundan M, Naqvi NI, Narendra DP, Narita M, Navarro M, Nawrocki ST, Nazarko TY, Nemchenko A, Netea MG, Neufeld TP, Ney PA, Nezis IP, Nguyen HP, Nie D, Nishino I, Nislow C, Nixon RA, Noda T, Noegel AA, Nogalska A, Noguchi S, Notterpek L, Novak I, Nozaki T, Nukina N, Nurnberger T, Nyfeler B, Obara K, Oberley TD, Oddo S, Ogawa M, Ohashi T, Okamoto K, Oleinick NL, Oliver FJ, Olsen LJ, Olsson S, Opota O, Osborne TF, Ostrander GK, Otsu K, Ou JH, Ouimet M, Overholtzer M, Ozpolat B, Paganetti P, Pagnini U, Pallet N, Palmer GE, Palumbo C, Pan T, Panaretakis T, Pandey UB, Papackova Z, Papassideri I, Paris I, Park J, Park OK, Parys JB, Parzych KR, Patschan S, Patterson C, Pattingre S, Pawelek JM, Peng J, Perlmutter DH, Perrotta I, Perry G, Pervaiz S, Peter M, Peters GJ, Petersen M, Petrovski G, Phang JM, Piacentini M, Pierre P, Pierrefite-Carle V, Pierron G, Pinkas-Kramarski R, Piras A, Piri N, Platanias LC, Poggeler S, Poirot M, Poletti A, Pous C, Pozuelo-Rubio M, Praetorius-Ibba M, Prasad A, Prescott M, Priault M, Produit-Zengaffinen N, Progulske-Fox A, Proikas-Cezanne T, Przedborski S, Przyklenk K, Puertollano R, Puyal J, Qian SB, Qin L, Qin ZH, Quaggin SE, Raben N, Rabinowich H, Rabkin SW, Rahman I, Rami A, Ramm G, Randall G, Randow F, Rao VA, Rathmell JC, Ravikumar B, Ray SK, Reed BH, Reed JC, Reggiori F, Regnier-Vigouroux A, Reichert AS, Reiners JJ, Jr, Reiter RJ, Ren J, Revuelta JL, Rhodes CJ, Ritis K, Rizzo E, Robbins J, Roberge M, Roca H, Roccheri MC, Rocchi S, Rodemann HP, Rodriguez de Cordoba S, Rohrer B, Roninson IB, Rosen K, Rost-Roszkowska MM, Rouis M, Rouschop KM, Rovetta F, Rubin BP, Rubinsztein DC, Ruckdeschel K, Rucker EB, 3rd, Rudich A, Rudolf E, Ruiz-Opazo N, Russo R, Rusten TE, Ryan KM, Ryter SW, Sabatini DM, Sadoshima J, Saha T, Saitoh T, Sakagami H, Sakai Y, Salekdeh GH, Salomoni P, Salvaterra PM, Salvesen G, Salvioli R, Sanchez AM, Sanchez-Alcazar JA, Sanchez-Prieto R, Sandri M, Sankar U, Sansanwal P, Santambrogio L, Saran S, Sarkar S, Sarwal M, Sasakawa C, Sasnauskiene A, Sass M, Sato K, Sato M, Schapira AH, Scharl M, Schatzl HM, Scheper W, Schiaffino S, Schneider C, Schneider ME, Schneider-Stock R, Schoenlein PV, Schorderet DF, Schuller C, Schwartz GK, Scorrano L, Sealy L, Seglen PO, Segura-Aguilar J, Seiliez I, Seleverstov O, Sell C, Seo JB, Separovic D, Setaluri V, Setoguchi T, Settembre C, Shacka JJ, Shanmugam M, Shapiro IM, Shaulian E, Shaw RJ, Shelhamer JH, Shen HM, Shen WC, Sheng ZH, Shi Y, Shibuya K, Shidoji Y, Shieh JJ, Shih CM, Shimada Y, Shimizu S, Shintani T, Shirihai OS, Shore GC, Sibirny AA, Sidhu SB, Sikorska B, Silva-Zacarin EC, Simmons A, Simon AK, Simon HU, Simone C, Simonsen A, Sinclair DA, Singh R, Sinha D, Sinicrope FA, Sirko A, Siu PM, Sivridis E, Skop V, Skulachev VP, Slack RS, Smaili SS, Smith DR, Soengas MS, Soldati T, Song X, Sood AK, Soong TW, Sotgia F, Spector SA, Spies CD, Springer W, Srinivasula SM, Stefanis L, Steffan JS, Stendel R, Stenmark H, Stephanou A, Stern ST, Sternberg C, Stork B, Stralfors P, Subauste CS, Sui X, Sulzer D, Sun J, Sun SY, Sun ZJ, Sung JJ, Suzuki K, Suzuki T, Swanson MS, Swanton C, Sweeney ST, Sy LK, Szabadkai G, Tabas I, Taegtmeyer H, Tafani M, Takacs-Vellai K, Takano Y, Takegawa K, Takemura G, Takeshita F, Talbot NJ, Tan KS, Tanaka K, Tang D, Tanida I, Tannous BA, Tavernarakis N, Taylor GS, Taylor GA, Taylor JP, Terada LS, Terman A, Tettamanti G, Thevissen K, Thompson CB, Thorburn A, Thumm M, Tian F, Tian Y, Tocchini-Valentini G, Tolkovsky AM, Tomino Y, Tonges L, Tooze SA, Tournier C, Tower J, Towns R, Trajkovic V, Travassos LH, Tsai TF, Tschan MP, Tsubata T, Tsung A, Turk B, Turner LS, Tyagi SC, Uchiyama Y, Ueno T, Umekawa M, Umemiya-Shirafuji R, Unni VK, Vaccaro MI, Valente EM, Van den Berghe G, van der Klei IJ, van Doorn W, van Dyk LF, van Egmond M, van Grunsven LA, Vandenabeele P, Vandenberghe WP, Vanhorebeek I, Vaquero EC, Velasco G, Vellai T, Vicencio JM, Vierstra RD, Vila M, Vindis C, Viola G, Viscomi MT, Voitsekhovskaja OV, von Haefen C, Votruba M, Wada K, Wade-Martins R, Walker CL, Walsh CM, Walter J, Wan XB, Wang A, Wang C, Wang D, Wang F, Wang G, Wang H, Wang HG, Wang HD, Wang J, Wang K, Wang M, Wang RC, Wang X, Wang YJ, Wang Y, Wang Z, Wang ZC, Wansink DG, Ward DM, Watada H, Waters SL, Webster P, Wei L, Weihl CC, Weiss WA, Welford SM, Wen LP, Whitehouse CA, Whitton JL, Whitworth AJ, Wileman T, Wiley JW, Wilkinson S, Willbold D, Williams RL, Williamson PR, Wouters BG, Wu C, Wu DC, Wu WK, Wyttenbach A, Xavier RJ, Xi Z, Xia P, Xiao G, Xie Z, Xu DZ, Xu J, Xu L, Xu X, Yamamoto A, Yamashina S, Yamashita M, Yan X, Yanagida M, Yang DS, Yang E, Yang JM, Yang SY, Yang W, Yang WY, Yang Z, Yao MC, Yao TP, Yeganeh B, Yen WL, Yin JJ, Yin XM, Yoo OJ, Yoon G, Yoon SY, Yorimitsu T, Yoshikawa Y, Yoshimori T, Yoshimoto K, You HJ, Youle RJ, Younes A, Yu L, Yu SW, Yu WH, Yuan ZM, Yue Z, Yun CH, Yuzaki M, Zabirnyk O, Silva-Zacarin E, Zacks D, Zacksenhaus E, Zaffaroni N, Zakeri Z, Zeh HJ, 3rd, Zeitlin SO, Zhang H, Zhang HL, Zhang J, Zhang JP, Zhang L, Zhang MY, Zhang XD, Zhao M, Zhao YF, Zhao Y, Zhao ZJ, Zheng X, Zhivotovsky B, Zhong Q, Zhou CZ, Zhu C, Zhu WG, Zhu XF, Zhu X, Zhu Y, Zoladek T, Zong WX, Zorzano A, Zschocke J, and Zuckerbraun B. Guidelines for the use and interpretation of assays for monitoring autophagy. *Autophagy* 8: 445–544, 2012.

51. **Kristensen AR, Schandorff S, Hoyer-Hansen M, Nielsen MO, Jaattela M, Dengjel J, Andersen JS.** Ordered organelle degradation during starvation-induced autophagy. *Mol Cell Proteomics* 7: 2419–2428, 2008.
52. **Kuma A, Matsui M, Mizushima N.** LC3, an autophagosome marker, can be incorporated into protein aggregates independent of autophagy: caution in the interpretation of LC3 localization. *Autophagy* 3: 323–328, 2007.
53. **Kume S, Uzu T, Horiike K, Chin-Kanasaki M, Isshiki K, Araki S, Sugimoto T, Haneda M, Kashiwagi A, Koya D.** Calorie restriction enhances cell adaptation to hypoxia through Sirt1-dependent mitochondrial autophagy in mouse aged kidney. *J Clin Invest* 120: 1043–1055, 2010.
54. **Lakka HM, Laaksonen DE, Lakka TA, Niskanen LK, Kumpusalo E, Tuomilehto J, Salonen JT.** The metabolic syndrome and total and cardiovascular disease mortality in middle-aged men. *JAMA* 288: 2709–2716, 2002.
55. **Lan F, Cacicedo JM, Ruderman N, Ido Y.** SIRT1 modulation of the acetylation status, cytosolic localization, and activity of LKB1. Possible role in AMP-activated protein kinase activation. *J Biol Chem* 283: 27628–27635, 2008.
56. **LaRocca TJ, Henson GD, Thorburn A, Sindler AL, Pierce GL, Seals DR.** Translational evidence that impaired autophagy contributes to arterial ageing. *J Physiol* 590: 3305–3316, 2012.
57. **Larsen PJ, Tennagels N.** On ceramides, other sphingolipids and impaired glucose homeostasis. *Mol Metab* 3: 252–260, 2014.
58. **Las G, Serada SB, Wikstrom JD, Twig G, Shirihai OS.** Fatty acids suppress autophagic turnover in beta-cells. *J Biol Chem* 286: 42534–42544, 2011.
59. **Lee IH, Cao L, Mostoslavsky R, Lombard DB, Liu J, Bruns NE, Tsokos M, Alt FW, Finkel T.** A role for the NAD-dependent deacetylase Sirt1 in the regulation of autophagy. *Proc Natl Acad Sci USA* 105: 3374–3379, 2008.
60. **Lee JW, Park S, Takahashi Y, Wang HG.** The association of AMPK with ULK1 regulates autophagy. *PLos One* 5: e15394, 2010.
61. **Li H, Min Q, Ouyang C, Lee J, He C, Zou MH, Xie Z.** AMPK activation prevents excess nutrient-induced hepatic lipid accumulation by inhibiting mTORC1 signaling and endoplasmic reticulum stress response. *Biochim Biophys Acta* 1842: 1844–1854, 2014.
62. **Li MF, Ren Y, Zhao CC, Zhang R, Li LX, Liu F, Lu JX, Tu YF, Zhao WJ, Bao YQ, Jia WP.** Prevalence and clinical characteristics of lower limb atherosclerotic lesions in newly diagnosed patients with ketosis-onset diabetes: a cross-sectional study. *Diabetol Metab Syndr* 6: 71, 2014.
63. **Loffler AS, Alers S, Dieterle AM, Keppeler H, Franz-Wachtel M, Kundu M, Campbell DG, Wesselborg S, Alessi DR, Stork B.** Ulk1-

mediated phosphorylation of AMPK constitutes a negative regulatory feedback loop. *Autophagy* 7: 696–706, 2011.
64. **Lu Y, Qian L, Zhang Q, Chen B, Gui L, Huang D, Chen G, Chen L.** Palmitate induces apoptosis in mouse aortic endothelial cells and endothelial dysfunction in mice fed high-calorie and high-cholesterol diets. *Life Sci* 92: 1165–1173, 2013.
65. **Martin KR, Xu Y, Looyenga BD, Davis RJ, Wu CL, Tremblay ML, Xu HE, MacKeigan JP.** Identification of PTPsigma as an autophagic phosphatase. *J Cell Sci* 124: 812–819, 2011.
66. **Merrill GF, Kurth EJ, Hardie DG, Winder WW.** AICA riboside increases AMP-activated protein kinase, fatty acid oxidation, and glucose uptake in rat muscle. *Am J Physiol Endocrinol Metab* 273: E1107–E1112, 1997.
67. **Miao F, Wu X, Zhang L, Yuan YC, Riggs AD, Natarajan R.** Genome-wide analysis of histone lysine methylation variations caused by diabetic conditions in human monocytes. *J Biol Chem* 282: 13854–13863, 2007.
68. **Miles JM, Wooldridge D, Grellner WJ, Windsor S, Isley WL, Klein S, Harris WS.** Nocturnal and postprandial free fatty acid kinetics in normal and type 2 diabetic subjects: effects of insulin sensitization therapy. *Diabetes* 52: 675–681, 2003.
69. **Mizushima N, Yamamoto A, Hatano M, Kobayashi Y, Kabeya Y, Suzuki K, Tokuhisa T, Ohsumi Y, Yoshimori T.** Dissection of autophagosome formation using Apg5-deficient mouse embryonic stem cells. *J Cell Biol* 152: 657–668, 2001.
70. **Mosbech MB, Kruse R, Harvald EB, Olsen AS, Gallego SF, Hannibal-Bach HK, Ejsing CS, Faergeman NJ.** Functional loss of two ceramide synthases elicits autophagy-dependent lifespan extension in *C. elegans*. *PLos One* 8: e70087, 2013.
71. **Nelson LE, Valentine RJ, Cacicedo JM, Gauthier MS, Ido Y, Ruderman NB.** A novel inverse relationship between metformin-triggered AMPK-SIRT1 signaling and p53 protein abundance in high glucose-exposed HepG2 cells. *Am J Physiol Cell Physiol* 303: C4–C13, 2012.
72. **Oh JM, Choi EK, Carp RI, Kim YS.** Oxidative stress impairs autophagic flux in prion protein-deficient hippocampal cells. *Autophagy* 8: 1448–1461, 2012.
73. **Paulson DJ, Crass MF 3rd.** Endogenous triacylglycerol metabolism in diabetic heart. *Am J Physiol Heart Circ Physiol* 242: H1084–H1094, 1982.
74. **Razani B, Feng C, Coleman T, Emanuel R, Wen H, Hwang S, Ting JP, Virgin HW, Kastan MB, Semenkovich CF.** Autophagy links inflammasomes to atherosclerotic progression. *Cell Metab* 15: 534–544, 2012.
75. **Reaven GM, Hollenbeck C, Jeng CY, Wu MS, Chen YD.** Measurement of plasma glucose, free fatty acid, lactate, and insulin for 24 h in patients with NIDDM. *Diabetes* 37: 1020–1024, 1988.
76. **Rodahl K, Miller HI, Issekutz B Jr.** Plasma free fatty acids in exercise. *J Appl Physiol* 19: 489–492, 1964.
77. **Sarwar N, Gao P, Seshasai SR, Gobin R, Kaptoge S, Di Angelantonio E, Ingelsson E, Lawlor DA, Selvin E, Stampfer M, Stehouwer CD, Lewington S, Pennells L, Thompson A, Sattar N, White IR, Ray KK, Danesh J.** Diabetes mellitus, fasting blood glucose concentration, and risk of vascular disease: a collaborative meta-analysis of 102 prospective studies. *Lancet* 375: 2215–2222, 2010.
78. **Scherz-Shouval R, Shvets E, Fass E, Shorer H, Gil L, Elazar Z.** Reactive oxygen species are essential for autophagy and specifically regulate the activity of Atg4. *EMBO J* 26: 1749–1760, 2007.
79. **Schneider CA.** Improving macrovascular outcomes in type 2 diabetes: Outcome studies in cardiovascular risk and metabolic control. *Curr Med Res Opin* 22, *Suppl* 2: S15–S26, 2006.
80. **Suchankova G, Nelson LE, Gerhart-Hines Z, Kelly M, Gauthier MS, Saha AK, Ido Y, Puigserver P, Ruderman NB.** Concurrent regulation of AMP-activated protein kinase and SIRT1 in mammalian cells. *Biochem Biophys Res Commun* 378: 836–841, 2009.
81. **Sullivan JE, Brocklehurst KJ, Marley AE, Carey F, Carling D, Beri RK.** Inhibition of lipolysis and lipogenesis in isolated rat adipocytes with AICAR, a cell-permeable activator of AMP-activated protein kinase. *FEBS Lett* 353: 33–36, 1994.
82. **Sun W, Lee TS, Zhu M, Gu C, Wang Y, Zhu Y, Shyy JY.** Statins activate AMP-activated protein kinase in vitro and in vivo. *Circulation* 114: 2655–2662, 2006.
83. **Takeda-Watanabe A, Kitada M, Kanasaki K, Koya D.** SIRT1 inactivation induces inflammation through the dysregulation of autophagy in human THP-1 cells. *Biochem Biophys Res Commun* 427: 191–196, 2012.
84. **Taniguchi M, Kitatani K, Kondo T, Hashimoto-Nishimura M, Asano S, Hayashi A, Mitsutake S, Igarashi Y, Umehara H, Takeya H, Kigawa J, Okazaki T.** Regulation of autophagy and its associated cell death by "sphingolipid rheostat": reciprocal role of ceramide and sphingosine 1-phosphate in the mammalian target of rapamycin pathway. *J Biol Chem* 287: 39898–39910, 2012.
85. **Vergne I, Roberts E, Elmaoued RA, Tosch V, Delgado MA, Proikas-Cezanne T, Laporte J, Deretic V.** Control of autophagy initiation by phosphoinositide 3-phosphatase Jumpy. *EMBO J* 28: 2244–2258, 2009.
86. **Wang Q, Zhang M, Liang B, Shirwany N, Zhu Y, Zou MH.** Activation of AMP-activated protein kinase is required for berberine-induced reduction of atherosclerosis in mice: the role of uncoupling protein 2. *PLos One* 6: e25436, 2011.
87. **Wang S, Song P, Zou MH.** AMP-activated protein kinase, stress responses and cardiovascular diseases. *Clin Sci (Lond)* 122: 555–573, 2012.
88. **Wen H, Gris D, Lei Y, Jha S, Zhang L, Huang MT, Brickey WJ, Ting JP.** Fatty acid-induced NLRP3-ASC inflammasome activation interferes with insulin signaling. *Nat Immunol* 12: 408–415, 2011.
89. **Wirth M, Joachim J, Tooze SA.** Autophagosome formation-The role of ULK1 and Beclin1-PI3KC3 complexes in setting the stage. *Semin Cancer Biol* 23: 301–309, 2013.
90. **Woods A, Azzout-Marniche D, Foretz M, Stein SC, Lemarchand P, Ferre P, Foufelle F, Carling D.** Characterization of the role of AMP-activated protein kinase in the regulation of glucose-activated gene expression using constitutively active and dominant negative forms of the kinase. *Mol Cell Biol* 20: 6704–6711, 2000.
91. **Wu Y, Song P, Xu J, Zhang M, Zou MH.** Activation of protein phosphatase 2A by palmitate inhibits AMP-activated protein kinase. *J Biol Chem* 282: 9777–9788, 2007.
92. **Xie Z, Nair U, Klionsky DJ.** Atg8 controls phagophore expansion during autophagosome formation. *Mol Biol Cell* 19: 3290–3298, 2008.
93. **Zhang H, Dellsperger KC, Zhang C.** The link between metabolic abnormalities and endothelial dysfunction in type 2 diabetes: an update. *Basic Res Cardiol* 107: 237, 2012.
94. **Zhang QJ, Holland WL, Wilson L, Tanner JM, Kearns D, Cahoon JM, Pettey D, Losee J, Duncan B, Gale D, Kowalski CA, Deeter N, Nichols A, Deesing M, Arrant C, Ruan T, Boehme C, McCamey DR, Rou J, Ambal K, Narra KK, Summers SA, Abel ED, Symons JD.** Ceramide mediates vascular dysfunction in diet-induced obesity by PP2A-mediated dephosphorylation of the eNOS-Akt complex. *Diabetes* 61: 1848–1859, 2013.
95. **Zhou G, Myers R, Li Y, Chen Y, Shen X, Fenyk-Melody J, Wu M, Ventre J, Doebber T, Fujii N, Musi N, Hirshman MF, Goodyear LJ, Moller DE.** Role of AMP-activated protein kinase in mechanism of metformin action. *J Clin Invest* 108: 1167–1174, 2001.